Early phenotypic asymmetry of sister oligodendrocyte progenitor cells after mitosis and its modulation by aging and extrinsic factors

Early phenotypic asymmetry of sister oligodendrocyte progenitor cells after mitosis and its modulation by aging and extrinsic factors

Enrica Boda[1], Silvia Di Maria[1], Patrizia Rosa[2], Verdon Taylor[3], Maria P. Abbracchio[4], Annalisa Buffo[1]

[1]Department of Neuroscience, Neuroscience Institute Cavalieri Ottolenghi (NICO), Università degli Studi di Torino, Regione Gonzole, 10 – 10043 Orbassano (Turin), Italy

[2]CNR- Institute of Neuroscience, Department of Medical Pharmacology, University of Milan, Italy

[3]Embryology and Stem Cell Biology, Department of Biomedicine, University of Basel, Mattenstrasse 28, CH-4058 Basel, Switzerland

[4]Laboratory of Molecular and Cellular Pharmacology of Purinergic Transmission – Department of Pharmacological and Biomolecular Sciences – Università degli Studi di Milano, via Balzaretti, 9 – 20133 Milan, Italy

Running title: Sister OPC asymmetry after mitosis

Number of words in:
Abstract: 202
Introduction: 527
Materials and Methods: 2046
Results: 2807
Discussion: 2022

Acknowledgements: 128
References: 1501
Figure legends: 1316
Number of Figures: 7 + 5 Supplementary figures
Number of Tables: 0
Total word count: 10552

Corresponding author:

Enrica Boda

Department of Neuroscience, Neuroscience Institute Cavalieri Ottolenghi (NICO), Università degli Studi di Torino, Regione Gonzole, 10 – 10043 Orbassano (Turin), Italy

enrica.boda@unito.it

Tel. 0039 011 6706630

Keywords: NG2 cells, asymmetry, division, maturation

Main points

A fraction of dividing OPCs generate sister cells with diverse immunophenotypic profiles and short-term fates in vivo. Such diversity emerges from the rapid downregulation of OPC markers and upregulation of molecules associated with lineage progression, rather than from their asymmetric segregation during mitosis. Fractions of symmetric/asymmetric sister OPC pairs varied with age and upon different pathophysiological conditions.

Abstract

Oligodendrocyte progenitor cells (OPCs) persist in the adult Central Nervous System and guarantee oligodendrocyte turnover throughout life. It remains obscure how OPCs avoid exhaustion during adulthood. Similar to stem cells, OPCs could self-maintain by undergoing asymmetric divisions generating a mixed progeny either keeping a progenitor phenotype or proceeding to differentiation. To address this issue, we examined the distribution of stage-specific markers in sister OPCs during mitosis and later after cell birth, and assessed its correlation with distinct short-term fates. In both the adult and juvenile cerebral cortex a fraction of dividing OPCs gives rise to sister cells with diverse immunophenotypic profiles and short-term behaviours. Such heterogeneity appears as cells exit cytokinesis, but does not derive from the asymmetric segregation of molecules such as NG2 or PDGFRa expressed in the mother cell. Rather, rapid downregulation of OPC markers and upregulation of molecules associated with lineage progression contributes to generate early sister OPC asymmetry. Analyses during aging and upon exposure to physiological (i.e. increased motor activity) and pathological (i.e. trauma or demyelination) stimuli showed that both intrinsic and environmental factors contribute to determine the fraction of symmetric and asymmetric OPC pairs and the phenotype of the OPC progeny as soon as cells exit mitosis.

Introduction

During Central Nervous System (CNS) ontogenesis, myelinating oligodendrocytes originate from neural progenitors expressing the platelet-derived growth factor alpha receptor (PDGFRa) and the NG2 chondroitin sulfate proteoglycan. After perinatal expansion by local proliferation, oligodendrocyte progenitor cells (OPCs) progressively differentiate into myelin-producing oligodendrocytes. However, OPCs persist in the adult CNS parenchyma, where they are continuously engaged into maturation to sustain the basal turnover and plasticity of myelin (Young et al., 2013; Hughes et al., 2013). This evidence raises the question of whether the OPC pool is maintained throughout the life of the organism and, if so, how. OPCs may undergo a progressive depletion over time, by stochastically differentiating after cycles of proliferation. Yet, OPC density is stable during adulthood and aging in the mouse CNS, indicating that the progenitor pool does not become exhausted (Rivers et al., 2008; van Wijngaarden and Franklin, 2013; see also Suppl. Fig.1). The persistence of OPCs could also be explained by a continuous replenishment by the germinal niches (i.e. the subventricular zone of the lateral ventricles and the subgranular zone of the hippocampus). However, in the intact brain under homeostatic conditions, oligodendrogenesis at these sites is very limited (Maki et al., 2013; Encinas et al., 2011) and migration of the niche-derived OPCs appears restricted to nearby white matter tracts (Agathou et al., 2013; Robins et al., 2013; Menn et al., 2006; Gonzalez-Perez et al., 2009). Hence, it seems very unlikely that niche activity can sustain OPC turnover throughout the CNS parenchyma. Alternatively, adult OPCs may self-maintain by mechanisms typical of stem cells, i.e. asymmetric cell division, based on the asymmetric segregation of specific molecules during mitosis (Knoblich, 2010) and resulting in the generation of a mixed cell progeny either keeping a progenitor/proliferative phenotype or proceeding to differentiation. In support of this view, a recent *in vitro* study reported that asymmetric inheritance of NG2 is required for the generation of cells with

distinct fates (Sugiarto et al., 2011), while *in vivo* and *in vitro* analyses showed that mixed clones are produced including immature cells and differentiated oligodendrocytes (Wren et al., 1992; Barres et al., 1994; Ibarrola et al., 1996; Sugiarto et al., 2011; Zhu et al., 2011; Nakatani et al., 2013). However, *in vivo* data on asymmetric mechanisms during mitosis are rare and often contradictory (Kukley et al., 2008; Sugiarto et al., 2011) and lack an association with fate. Further, it remains unaddressed whether the modality of OPC division may be affected by extrinsic environmental factors.

To tackle these issues we examined *in vivo*: i) the distribution of progenitor and maturational markers in sister OPCs during mitosis and at later time points, and the correlation between marker expression and distinct early fates; and ii) alterations in marker distribution during aging as well as upon exposure to physiological and pathological stimuli. We found sister OPCs with diverse immunophenotypic profiles and short-term fates. Results also indicate that, rather than segregation during mitosis, downregulation of progenitor markers and upregulation of molecules associated with lineage progression at the exit of the cell cycle contribute to generate sister OPC asymmetry. Finally, we show that environmental factors significantly affect the immunophenotypic profile of sister OPCs as early as cells exit mitosis.

Materials and methods

Animals

All experimental procedures were performed on C57BL/6 mice. Surgery and perfusions were carried out under deep general anaesthesia (ketamine, 100 mg/kg; Ketavet, Bayern, Leverkusen,Germany; xylazine, 5 mg/kg; Rompun; Bayer, Milan,Italy). The experimental plan was designed according to the guidelines of the NIH, the European Communities Council (2010/63/EU) and the Italian Law for Care and Use of Experimental Animals (DL116/92). It was also approved by the Italian Ministry of Health and the Bioethical Committee of the University of Turin. Cortical stab-wound and lysolecithin-induced focal demyelination were performed as described in Boda et al., 2011. For voluntary physical exercise experiments, adult (2-4 months old) mice were housed in cages equipped with running wheels for 2 weeks, while control animals were housed in standard conditions. Hes5-GFP (Lugert et al., 2010) and NG2creER^{TM};R26YFP mice (Zhu et al., 2011; Srinivas et al., 2001) were used to monitor respectively Hes5 expression or NG2 promoter activity in newly generated cells (see Suppl. Fig. 2A and below). Juvenile (postnatal day 20, P20) p53 knock-out (KO; Jacks et al., 1994) mice and age-matched wild-type littermates were used to investigate the phenotype of OPC progeny in a context of reduced oligodendrocyte cell death (Eizenberg et al., 1995; Li et al., 2008). For long-term pair analysis (see below) in adult cortex we used NestinCreERT2;R26YFP mice (Corsini et al., 2009; Srinivas et al., 2001). Cre activity and YFP reporter expression were induced in NG2creER^{TM};R26YFP and NestinCreERT2;R26YFP mice by oral administration of tamoxifen (Sigma-Aldrich, Milan, Italy) dissolved in corn oil (5 mg by oral gavage for two consecutive days; see also Suppl. Fig. 2A).

OPC pair analysis

To study the early phenotype of pairs of sister OPCs, we employed the thymidine analogue 5-bromo-2-deoxyuridine (BrdU, Sigma Aldrich) that is incorporated in the DNA during the S-phase of the cell cycle and is then inherited by daughter cells. Two subsequent BrdU injections (100 mg/kg body weight for adult mice or 50 mg/kg body weight for pups, i.p.) were performed at a 2 hours distance. Distinct cohorts of animals were sacrificed at 2 hours, 1, 7, 16 or 30 days after the last pulse (see Suppl. Fig. 2A). Virtually all (more than 95%) BrdU-incorporating cells detected at 2 hpi (hours post-last BrdU injection) in the intact juvenile (P20) and adult cortex were NG2+/PDGFRa+ double-labeled OPCs. Olig2 positivity was also confirmed, in line with the oligodendroglial nature of these proliferative cells (not shown). At this stage, virtually all (93.9 ± 7.1%) BrdU+ OPCs appeared as isolated cells (i.e. > 50 μm apart), while at 1 dpi (day post-BrdU injection) the vast majority (87.4 ± 3.9 %) of BrdU-retaining cells were detected as pairs and the total number of BrdU+ cells increased by 2.2 folds, indicating the division of cells that had formerly incorporated BrdU. Very few BrdU+ OPC pairs were labeled by this approach in the adult and juvenile cortex (see also Fig. 7). BrdU+ nuclei were considered as sister cells if they: i) were their closest BrdU+ partners; ii) showed similar intensity and configuration of BrdU labeling; iii) displayed similar configuration of the chromatin (see also below); iv) showed mirror morphologies (at short time points after division); iv) their distance (from middle to middle of the nuclei) was below 34.7 ± 2 μm, which is the minimal average distance between NG2+ cell nuclei in the cortical parenchyma. This latter criterion allowed to distinguish sister cells from duplets of unrelated OPCs that randomly occurred to incorporate BrdU at the same time (see also Kukley et al., 2008). Of note, at 1 dpi cells appeared closer than 10 μm (distance from the middle of the nuclei) in more than 97% of BrdU+ OPC pairs in both juvenile and adult cortices. The distance between newborn sister cells progressively increased at later time points. In the adult brain at 30 dpi, about 20% of

the OPC pairs were excluded from the analysis due to cell dispersion (more than 30 μm apart). Isolated cells (e.g. about 13% of all Olig2+/BrdU+ in the juvenile cortex) were excluded from analysis.

To investigate the NG2 promoter activity in newly generated OPC pairs, mice were given tamoxifen at 1 and 2 dpi and then sacrificed after 2 weeks (Suppl. Fig. 2A). To study the early phenotype of OPC sister cells generated upon traumatic or demyelinating injury, mice were given BrdU at 3 days after lesion (dpl) and then sacrificed at 4 dpl (Suppl. Fig. 2A). Analogously, to characterize sister OPCs born in conditions of increased physical exercise, BrdU injections followed 2 weeks of unlimited access to running wheels and mice were sacrificed at 1 dpi. To label cells re-entering cell cycle in the juvenile cortex, BrdU was administered at P20, then a second thymidine analogue (5-ethynyl-2'-deoxyuridine, EdU; Molecular Probes) was injected once (50 mg/kg body weight, i.p.) at 7 dpi and mice were sacrificed after a 2 hour period of chase. OPC pair phenotype was studied by combing anti-BrdU staining with immunolabeling directed against different antigens (see below) and evaluating the percentage of marker expression on the whole number of BrdU+ pairs in the juvenile and adult cortex or of BrdU+/Olig2+ double labeled pairs in those conditions where OPCs accounted only for a fraction of BrdU-incorporating cells (i.e. 77% at P10, 70% at 4 days after stab-wound and 60% at 4 days after lysolecithin injection).

For long-term analysis of OPC pairs, we took advantage of the NestinCreERT2;R26YFP mouse line, where Cre recombination occurs in the germinal niches and in a fraction of parenchymal proliferating and newly-generated OPCs, consistent with earlier findings in Nestin-eGFP mice (Walker et al., 2010). Accordingly, at 7 days post-tamoxifen injection, pairs of YFP+ juxtaposed OPCs decorated the cortical tissue (Fig. 5A). YFP+ OPC pairs/clusters were considered as clones only if they were separated from other YFP+

pairs/clusters by more than 50 μm, consistent with criteria used for previous OPC clonal analysis (Zhu et al., 2011).

For both BrdU- and NestinCreERT2;R26YFP- based pair analyses, we routinely scanned the entire cortical grey matter included in slices from Bregma 1.10 to Bregma -2.00 (and corresponding levels in the postnatal brain). With the exception of the lysolecithin-induced demyelination, analyses were performed on grey matter to avoid possible contributions of SVZ-derived OPCs. Unless otherwise indicated, at least 100 OPC pairs were inspected.

Histological analysis

For histological analysis, animals were anaesthetized (as above) and transcardially perfused with 4% paraformaldehyde (PFA) in 0.1M phosphate buffer (PB). Brains were post-fixed for 2 hours, cryoprotected, and processed according to standard protocols (Buffo et al., 2005). Brains were cut in 50 μm thick coronal sections collected in PBS and then stained to detect the expression of different antigens: NG2 (1:200, Millipore); PDGRa (1:300, BD); Sox2 (1:200, Santa Cruz); PLP/DM20 (1:5, kind gift of B. Zalc, INSERM, Paris); Nkx2.2 (1:100, Developmental Studies Hybridoma Bank); GST-pi (1:500, Eppendorf); GFP (1:700, Invitrogen); BrdU (1:500, Abcam); LMNB1 (1:500, Abcam); Olig2 (1:500, Millipore). GPR17 was detected by means of affinity-purified antibodies (1:100; Ciana et al., 2006; Boda et al., 2011). Incubation with primary antibodies was made overnight at 4°C in PBS with 0.5% Triton-X 100. The sections were then exposed for 2 h at room temperature (RT) to secondary Cy3- (Jackson ImmunoResearch Laboratories, West Grove, PA) and Alexafluor- (Molecular Probes Inc, Eugene Oregon) conjugated antibodies (Boda et al., 2011). 4,6-diamidino-2-phenylindole (DAPI, Fluka, Milan, Italy) was used to counterstain cell nuclei. After processing, sections were mounted on microscope slides with Tris-glycerol supplemented with 10% Mowiol (Calbiochem,LaJolla, CA). For colabeling of primary antibodies developed in the same species, the high sensitivity

tyramide signal amplification kit (Perkin Elmer, Monza, Italy) was utilized according to the manufacturer's instruction (see also Buffo et al., 2005). Stainings for PLP/DM20 and Nkx2.2 were preceded by antigen retrieval (5 minutes in citrate buffer pH 6 at 95°C). To allow BrdU recognition, slices were treated with 2N HCl for 20 min at 37°C, followed by 10 min in borate buffer before adding primary antibodies. EdU incorporation was visualized by means of the Click-iT EdU AlexaFluor633 HCS Assay (Life Technologies, Monza, Italy).

Analysis of the mitotic figures

Distinct OPC mitotic phases in the juvenile mouse cortex were distinguished as described in (Kukley et al., 2008), based on DNA (DAPI) organization and nuclear envelope (labeled by anti-LMNB1 staining) appearance. Cells undergoing prophase showed chromatin compaction in grains and initial disorganization of the nuclear envelope. Metaphase corresponded to accumulation of highly condensed DNA along the metaphasic plate. OPCs in anaphase displayed highly condensed chromatin distributed at the two poles, but still included in a unique nuclear envelope. Telophase appeared rather similar to anaphase (i.e. highly condensed chromatin distributed at the two poles) but showed formation of a membranous PDGFRa- and NG2- enriched septum between the two prospective daughter cells. Cells that just exited cytokinesis showed juxtaposed and specular cell somata with decondensing grainy DNA.

Primary OPC cultures

Primary oligodendrocyte precursors were isolated from mixed glial cultures from P2 Wistar rat cortex, by shaking method, as described in Fumagalli et al., 2011. OPCs were plated at clonal density onto poly-D-lysine (1μg/ml, Sigma-Aldrich, Milan, Italy) coated glass coverslips for immunocytochemistry in Neurobasal with 1X B27 (Invitrogen, Milan, Italy), 2 mM L-glutamine and either i) 10 ng/ml human platelet-derived growth factor (PDGF)-BB; ii)

10ng/ml PDGF-BB and 10ng/ml human basic fibroblast growth factor (bFGF); iii) 20ng/ml epidermal growth factor (EGF) and 20ng/ml bFGF(see Suppl. Fig. 2B). Growth factors were purchased from Miltenyi Biotec (Calderara di Reno, Italy). After one day, cells were fixed for 20 minutes at RT with 4% PFA in 0.1 M PB and labeled with anti-O4 primary antibody (1:100, Millipore) overnight at 4°C in PBS, then incubated for 1 hour RT with anti-mouse IgM Cy3-conjugated secondary antibody (Jackson ImmunoResearch Laboratories). After 5 minute incubation in 2% PFA, coverslips were then labeled with anti-NG2 antibody (1:500, Millipore) in PBS with 0.25% Triton-X 100 for 2 hours at RT and then incubated with Alexa488-conjugated secondary antibody (Molecular Probes) for 1 hour RT. After a 5 minute incubation with DAPI (1:1000), coverslips were finally mounted with Tris-glycerol supplemented with 10% Mowiol (Calbiochem).

OPC isolation and RT-PCR

Cell isolation and RT-PCR were performed as described in Rolando et al., 2012. Briefly, cerebral cortices of 6-8 P8 or P21 mice were dissected and dissociated using Neural Tissue Dissociation kit (Miltenyi Biotec). OPCs were enriched by positive selection using anti-AN2 or anti-PDGFRa (kind gift of Miltenyi Biotec) antibodies conjugated to magnetic beads, according to the instructions of the manufacturers (Miltenyi Biotec). Purity of the selected cells was verified by both immunocytochemistry (more than 94% of the cells were NG2+); and by performing RT-PCR experiments to exclude the expression of neuronal and astroglial markers, such as neurofilament-M, FW: (5')TAGAGCGCAAAGATTACCTGAAG (3'); RV: (5')TTGACGTTAAGGAGATCCTGGTA (3') or BLBP, FW: (5')TGAGTACATG AAAGCTCTGGGCGT(3'); RV: (5')TGAGCTTGTCT CCATCCAACCGAA(3'). Primers used were the following: mNUMB, FW: (5')CTTGTGTTCCCAGATCACCAG(3'); RV: (5')CCGCACACTCTTTGACACTTC(3'); Dll1, FW: (5')CTGAGGTGTAAGATGGAAGCG (3'); RV: (5') CAACTGTCCATAGTGCAATGG

(3'); Stau2, FW: (5') GTGTTTGAGATT GCGCTGAA(3'); RV: (5') TGCATTACGAACTCTCGACG(3'); Dyrk1A, FW: (5')TGACATCCCTGTCTTCCTCA (3'); RV: (5') TCCATTCTGTCCAAAGTCCA(3') (Ferron et al., 2010); AspM, FW: (5') TTTCGCAGCAACACTCATTC (3'); RV: (5') AGAGTAGCAGCCAGGTGCAT(3'); Trim32, FW: (5') GAAAGCAGGACCTCTTGACG(3'); RV: (5') ATATGTTCCCGTCTGCCTTG(3'); Par3, FW: (5') CAGACTCAAGGCAGGAGACC (3'); RV: (5') GGGTGTGAGAACAACGTCCT(3'); PDGFRa, FW: (5')TGGCATGATGGTCGATTCTA(3'); RV: (5')CGCTGAGGTGGTAGAAGGAG(3'); bActin, FW: (5') AGGCACCAGGGTGTGATGGT(3'); RV: (5') TGGCTGGGGTGTTGAAGGTC(3'). Amplifications followed this protocol: 35 cycles, each cycle with 95°C for 30 s, 58°C for 1 min, 72°C for 30 s, after an initial denaturation at 95°C for 3 min.

Image Processing and Data Analysis

Histological specimens were examined using an E-800 Nikon microscope (Nikon, Melville, NY) connected to a colour CCD Camera and a Leica TCS SP5 (Leica Microsystems, Wetzlar, Germany) confocal microscope. Adobe Photoshop 6.0 (Adobe Systems, San Jose, CA) was used to adjust image contrast and assemble the final plates. Quantitative evaluations (OPC pair densities, marker coexpression) were performed by confocal analysis or by means of the Neurolucida software (MicroBrightfield, Colchester, VT). Measurements derived from 5-10 sections per animal. Three to five animals were analyzed for each time point or experimental condition. Statistical analyses were carried out by the SigmaStat software package (Jandel Scientific, Germany) and included one-way ANOVA test (to compare mean values) followed by Bonferroni's post hoc analysis, unpaired Student's t test (when comparing only two groups), Chi-square test (to compare frequencies). Percentages were treated according to the arcsin transformation. In all

instances, $P < 0.05$ was considered as statistically significant. Data were expressed as averages ± standard deviations (SD).

Results

Markers associated with the progenitor phenotype or cell cycle exit are asymmetrically expressed in pairs of sister OPCs early after cell division

To assess whether OPCs undergo asymmetric cell division in juvenile (P20) and adult mice, we labeled cycling cells and their progeny by BrdU incorporation and investigated their phenotype 1 day post-BrdU injection (dpi; see Methods and Suppl. Fig. 2 for methodological details). We used NG2, PDGFRa and Sox2 as markers typical of immature OPC and proliferative stages (Hill and Nishiyama, 2014 ; Lee et al., 2013). In the cortical parenchyma of Hes5-GFP mice (Lugert et al., 2010), GFP decorates many astrocytes and some OPCs (about 10% of all GFP+ cells at P20; see Fig. 1J-L). We used this model to monitor the activation of the canonical Notch pathway, indicative of the maintenance of an early progenitor phenotype (Liu et al., 2006; Kondo and Raff, 2000). Expression of the GPR17 receptor, the transcription factor Nkx2.2 and PLP/DM20 (the immature splice variant of the myelin protein PLP) were used to mark non-mitotic OPCs and premyelinating stages (Boda et al., 2011; Nakatani et al., 2013; Zhu et al., 2014; Kukley, et al., 2010; see also Suppl. Fig. 3). Notably, at 1 dpi Nkx2.2 and PLP/DM20 were almost absent in newly generated OPCs (they decorated less than 2% of BrdU+ OPC pairs, not shown). Conversely, all other markers defined three types of BrdU+ OPC pairs: pairs where both sister OPCs expressed the markers (Fig. 1A, D, G, J, M), pairs where both sister OPCs were marker-negative (Fig. 1C, F, I, L, O) and pairs where markers were asymmetrically distributed in only one of the two sister cells (Fig 1B, E, H, K, N). This last fraction is consistent with the production of distinct daughter cells from the same mother OPC. The asymmetric fractions were rather broad for NG2 and PDGFRa (30-35% at both P20 and adult ages, Fig. 1 P,Q), which decorated the large majority of neogenerated OPCs (PDGFRa 76.5 ± 6.1% at P20, 64.1 ± 8.7 % at 2 months; NG2 78.2 ± 7.5% at P20, 70.51 ± 5.3% at 2 months). The asymmetric fractions were more discrete for Sox2 and Hes5

positivities (about 15% of all OPC pairs; Fig. 1Q), in line with an overall more restricted expression of these factors in newly produced cells (28.6 ± 4.2% Sox2; 29.4 ± 5.1% Hes5-GFP at P20). Asymmetric GPR17 distribution also appeared as intracellular Golgi-like accumulations (indicative of the early activation of receptor biosynthesis; Boda et al., 2011) in about 30% of pairs of OPC sister cells (Fig. 1 P,Q).

As a next step, we asked whether marker distribution was random or consistently defined daughter cells either keeping or losing progenitor features. In the juvenile cortex PDGFRa largely overlapped with GPR17 in newly generated cells (77.6 ± 4.5% of the GPR17+/BrdU+ cells were PDGFRa+). However, GPR17+ cells comprised only one third (32.1 ± 6%) of the newborn PDGFRa+ cells, in line with an early heterogeneity in the OPC progeny (Fig. 1R). Conversely, 83.1 ± 10.9 % of newly generated GPR17+ cells were Sox2 negative (Fig. 1R) and, in duplets asymmetric for GPR17, Sox2 appeared in the GPR17-negative sister cell 5-fold more frequently than in the GPR17+ one (Fig. 1S). Thus, at 1 dpi the large majority of newborn OPCs express PDGFRa. Within this pool, Sox2 and GPR17 mark two distinct cell subsets, suggesting an early phenotype distinction.

In further support of the existence of a precocious phenotypic heterogeneity in a subset of sister OPCs, we found that the NG2 promoter activity was differentially regulated early after mitosis. When Cre recombinase activity was induced in adult NG2creER™; R26YFP mice (Zhu et al., 2011; Srinivas et al., 2001) on the first and second day after BrdU administration and brains were analysed after 2 weeks, YFP expression was found asymmetrically distributed in 20.8 ± 4.7% of BrdU+ OPC pairs (Fig. 2C). Notably, within YFP-asymmetric pairs, GPR17 appeared 7-fold more frequently in YFP-negative cells than in the YFP-positive ones (43.2 ± 5.6% vs. 7.1 ± 1.7% of cases; Fig. 2D), while PDGFRa-positivity displayed a complementary pattern (9.2 ± 1.2% vs. 50.1 ± 6.3% of cases; Fig. 2E). This indicates consistent phenotypic differences in YFP+ and negative sister cells and excludes that YFP asymmetry reflects only a partial recombination efficiency of the

NG2creER™;R26YFP mouse line. On the whole, these data indicate that in both the adult and late postnatal cortex a fraction of cycling OPCs gives rise to a progeny that appears endowed with distinct properties immediately after cell division.

Newborn sister OPCs with distinct immunophenotypic profiles have different short-term fates

To assess whether the early asymmetric features detected in sister OPCs are maintained at later time points and associate with distinct cell fates, we examined marker expression and proliferation of BrdU-retaining sister OPCs at 7 dpi. This analysis was performed on juvenile cortices to take advantage of the relatively fast kinetics of both proliferation and differentiation, typical of this age (Zhu et al., 2011). Notably, at 7 dpi the number of BrdU-retaining Olig2+ cell pairs did not significantly differ from that at 1dpi (not shown). Among them the expression of the progenitor markers NG2, PDGFRa and Hes5 appeared significantly reduced ($P<0.01$ for PDGFRa, $P<0.001$ for NG2 and Hes5-GFP, Chi-square test, compare Fig. 1Q and Fig. 3A). Conversely, the fractions of Olig2+/BrdU+ pairs symmetrically or asymmetrically expressing Sox2 or GPR17 did not differ from those found at 1 dpi ($P>0.05$, Chi-square test, compare Fig. 1Q and Fig. 3A). Yet, at this stage the receptor appeared highly upregulated and localized in both cell somata and processes (Fig. 3D,E), indicating a progression in the lineage (Boda et al., 2011). Further, the maturation markers Nkx2.2 and PLP/DM20 were detected in a relevant fraction of BrdU+ cells (about 30% and 20%, respectively) and appeared with either symmetric or asymmetric distributions in cell pairs (Fig. 3A).

Notably, at 7dpi PDGFRa expression was clearly more segregated from GPR17 compared to 1dpi. PDGFRa expression decreased to 39.1 ± 9.1% of the GPR17+/BrdU+ OPCs, while it was found in about 75% of the GPR17-negative BrdU+ cells (Fig. 3B). On the contrary, 75 ± 9.2% and 33.1 ± 4.3% of the GPR17+ BrdU-retaining cells coexpressed

Nkx2.2 and PLP/DM20, respectively. The two markers were instead detected in less than 10% of the GPR17-negative/BrdU+ cells (Fig. 3B). Notably, when GPR17 appeared heterogeneously expressed within a pair, Nkx2.2 and PLP/DM20 colocalized with the receptor with relevant frequency (Fig 3C, E), while they were never found in GPR17-negative sister cells (Fig. 3C). Conversely, within this class of pairs, PDGFRa clearly prevailed in GPR17-negative OPCs (Fig. 3C, E). These data indicate that distinct features detected in OPC sister cells at 1dpi are maintained at 7 dpi and identify subsets either acquiring premyelinating markers or keeping a progenitor phenotype. To determine whether cell proliferation occurred in either cell types or not, we labelled cells re-entering cell cycle by administering a second thymidine analog (EdU) at 7dpi and analyzed BrdU/EdU colocalization within OPC pairs after a 2 hour chase period (see Methods and Suppl. Fig. 2). With this approach, we found BrdU-retaining cell pairs where both (about 30% of all BrdU+ pairs) or none (about 65%) of the sister cells had incorporated EdU (Fig. 4A, B). Most notably, we also detected pairs where only one sister OPC appeared BrdU-/EdU- double labelled (about 16% of the re-proliferating BrdU+ OPC pairs, corresponding to 5.6 ± 1.9 % of all BrdU-retaining pairs; n=253; Fig. 4C,D), indicating asymmetric S-phase entry among the OPC progeny. Notably, similar to what found at later time points in adult mice (see below and Fig. 5D), at this stage about 10% of BrdU-retaining clones appeared to contain three nearby cells (Fig. 4E), likely derived by the division of only one sister OPC within a pair. Of note, cells re-entering cell cycle never displayed GPR17 (Fig. 4D,F). Rather, at this time point high levels of the nuclear protein p27kip1 decorated GPR17-expressing cells in pairs, further suggesting exit from the cell cycle and entrance in a non-mitotic phase (Durand and Raff, 2000, Fig. 4G). Consistently, 90% of BrdU+ triplets were composed of two PDGFRa+/GPR17-negative cells and one PDGFRa-negative/GPR17+ cell (n= 25 out of 28 triplets). On the whole, these data show that in sister cells the persistence of a progenitor phenotype associates with the potential to re-

enter cell cycle, whereas cells expressing GPR17 enter a non-mitotic phase and acquire premyelinating markers.

Asymmetry in sister OPCs persists for months in the adult brain

Then, we investigated the phenotype of adult BrdU-retaining OPCs after longer chases to assess whether the heterogeneity found at short time points after division occurred also later. Notably, within the adult mouse cortex at 16 and 30 dpi about one third of the BrdU+ OPC pairs displayed a heterogenous expression of GPR17 (Suppl. Fig. 4). This long term asymmetry was also confirmed in NestinCreERT2;R26YFP mice (Corsini et al., 2009; Srinivas et al., 2001), where tamoxifen-induced Cre recombination occurs in cycling OPCs in the cortical parenchyma and permanently labels the OPC progeny (Fig. 5A). The NestinCreERT2 mouse line appeared a more suitable model for long term OPC pair analysis compared to NG2CreERTM;R26YFP mice, where recombination occurs in both proliferative and quiescent OPCs. At 5 weeks post-tamoxifen administration, GPR17 was asymmetrically expressed in only one sister cell in a large fraction of YFP+ pairs (41.2 ± 7.5%). Here, the receptor appeared distributed in both the soma and processes, consistent with pair generation at earlier time points (Boda et al., 2011; Fig. 5C). Interestingly, YFP+ OPC clusters including three nearby cells were also found (Fig. 5E), indicative of re-proliferation of only one between two sister cells. Later on, at 11 weeks post-tamoxifen administration, we still detected YFP+ pairs with asymmetric marker expression and morphology. In particular, pairs were rather frequent where one sister cell with a round cell body expressed glutathione-S-transferase (GST)-pi, a marker of mature and myelinating oligodendrocytes (Tamura et al., 2007; Fig. 5F), while the other GST-pi negative cell displayed a typical OPC morphology with extended YFP+ ramifications (Fig. 5F). Thus, phenotypic asymmetry in sister OPCs does not vanish with time, but can be observed in cells likely generated several weeks earlier.

Markers of progenitor state or cell cycle exit during mitosis

So far results showed that sister cells in OPC pairs display early asymmetric features that are related to distinct behaviours. However, it remained to be clarified whether this heterogeneity is produced during mitosis, as would occur for conventional asymmetric divisions similar to those in stem cells. To address this issue we examined NG2 and PDGFRa distribution during mitosis. Different mitotic phases in P20 mouse cerebral cortex were distinguished based on DNA and nuclear envelope appearance (see Methods and Kukley et al., 2008 for the criteria used to categorized mitotic configurations). As expected, 100% of OPCs undergoing prophase (Fig. 6A,B; n=95 on three mice) or metaphase (Fig. 6C,D; n=86 on three mice) displayed high levels of both PDGFRa (Fig. 6A,C) and NG2 (Fig. 6B,D) and never coexpressed GPR17 (Fig. 6A,C,D). Further, OPCs in anaphase or telophase still showed a homogenous expression of both PDGFRa and NG2 (Fig. 6E-G; n=98 on three mice), indicating absence of segregation *in vivo*. However, at the end of cytokinesis pairs of juxtaposed sister cells with de-condensing DNA were detected with uneven levels of NG2 (Fig. 6I) or PDGFRa (18% of OPC pairs, Fig. 6K; n= 148). Consistently, about 20% of the first BrdU+ OPC pairs appearing 4 hours after the S-phase entry (4hpi) showed an asymmetric expression of PDGFRa in the two sister cells (Fig. 6L). Similar results were obtained *in vitro* when we investigated the distribution of NG2 in mitotic OPCs cultivated for 24h at clonal density in EGF+bFGF, PDGF+ bFGF or PDGF alone (see Methods and Suppl. Fig. 2). These media differently affect cell maturation and preserve proliferation (Sugiarto et al., 2011; Sohn et al., 2006). Hence, they could differentially influence mitotic asymmetry. In none of the conditions we found asymmetric segregation of NG2 during mitosis (Fig. 6M-Q). Rather, in a subset of pairs, NG2 appeared clustered in intracellular endosome-like vesicles (Fig. 6R,S), suggesting it was undergoing degradation. Notably, such cytoplasmic NG2+ accumulations occasionally were

asymmetrically distributed in dividing OPCs in telophase (Fig. 6S), indicating that, similar to what we observed *in vivo*, sister OPC asymmetry occurred by NG2 downregulation in cells exiting mitosis *in vitro*. Thus, diversity in the expression of NG2 and PDGFRa in sister OPCs is induced starting from the end of cell division by a mechanism of downregulation rather than through their asymmetric distribution in daughter cells during mitosis.

When GPR17 expression was examined, we detected intracellular GPR17+ accumulations in a fraction of OPCs as early as in telophase (Fig. 6F,G). Such spots were reminiscent of Golgi vesicles (see also Boda et al., 2011) and were frequently found distributed in only one of the two prospective daughter cells (Fig. 6F,G). Further, GPR17 appeared asymmetrically distributed in about 15% of the OPC pairs that just exited cytokinesis (n=148; Fig. 6H,I). Consistently, about 25% of the BrdU+ OPC pairs found at 4hpi expressed the receptor in both or in only one of the two daughter cells (Fig. 6L). These data show that heterogeneity in sister cells appears a result of up- or down-regulation processes starting during the last phases of mitosis.

Intrinsic and extrinsic factors influence early heterogeneity of sister OPCs in vivo

Asymmetry after mitosis is reportedly regulated by both intrinsic and extrinsic factors acting in dividing neural progenitors (Lu et al., 2000). Thus, we asked whether the probability for a cycling OPC to generate daughter cells with early symmetric/asymmetric features might vary at different ages or upon distinct physiological and pathological stimuli. To address this issue we studied the phenotype (PDGFRa and GPR17 expression) of BrdU-retaining OPC duplets at 1 dpi: i) at postnatal *vs.* adult vs. old age; ii) in intact *vs.* injury conditions; iii) in standard conditions *vs.* after increased motor activity; iv) in WT *vs.* p53-KO mouse cortex (see Methods and Suppl. Fig.2).

The frequencies of symmetric/asymmetric pairs significantly varied with age (Fig. 7A-C), in parallel with a progressive decline in the number of newly generated OPC pairs ($P<0.001$;

One-way Anova F=31.52; R^2=0.9). In particular, the asymmetric fractions for either PDGFRa or GPR17 expression increased in the transition from early postnatal to adult stages (P<0.05 P20 *vs*. 2 months for both PDGFRa and GPR17, One-way Anova F=14.79 R^2=0.72 and F=13.22 R^2=0.83; Fig. 7B,C). Conversely, in older mice this trend was not confirmed, due to the enlargment of the symmetric PDGFRa double positive and GFPR17 double negative fractions (P<0.05 2 months *vs.* 12 months old for both, t-test; Fig. 7B,C). These data may reflect an enhancement of asymmetric mechanisms in the adult brain and the progressive lowering of OPC differentiation potential during aging (van Wijngaarden and Franklin, 2013).

When reacting to traumatic injury (stab-wound) or focal demyelination (lysolecithin toxicity) (see Methods and Suppl. Fig. 2 for experimental details), OPC proliferation markedly increased (P<0.01; SW or LPC *vs.* intact, t-test; Fig. 7D,F). Further, the GPR17 symmetric fraction expanded at the expenses of the double-negative fraction (P<0.001, SW and LPC *vs*. intact; t-test; Fig. 7E,G) while the frequency of asymmetric duplets remained stable. Of note, while in the intact cortex at 1 dpi the receptor appeared clustered in intracellular Golgi-like accumulations (Fig. 1M,N), in both lesion paradigms it was distributed in both somata and processes of most newborn GPR17-expressing cells (61.57 ± 16.1%; not. shown). Thus, overall injury-related signals appear to rapidly trigger the upregulation of molecules associated with cell cycle exit and possibly lineage progression.

Voluntary physical exercise has been reported to enhance OPC differentiation and decrease proliferation (Simon et al., 2011; see also Fig. 7H). In this experimental model, we observed a significant increase of the GPR17 asymmetric fraction and a reduction of the double negative subset (P<0.05; running vs. standard conditions, t-test, Fig. 7I). This indicates that physiological variations in neuronal activity modulate the OPC fate as early as during mitosis, and suggests that asymmetric mechanisms may sustain progenitor maintenance in this experimental condition.

Interestingly, these variations are not a stereotyped response to decreased proliferation. In juvenile p53 knock-out (KO) mice, where oligodendrocyte death is reduced by p53 ablation (Eizenberg et al., 1995; Li et al., 2008) and little proliferation occurs (Fig. 7L), the symmetric GPR17 fraction decreased by half, in parallel with an expansion of the negative cells ($P<0.05$, p53-KO vs. WT, t-test; Fig. 7J). This pattern may reflect a response to decreased needs for replacement. Notably, in all experimental models PDGFRa distribution in newborn OPC pairs did not vary significantly compared to control conditions (not shown; $P>0.05$ for all conditions vs. control; Chi-square-test).

On the whole, these results indicate that the probability for a cycling OPC to generate a progeny exiting the cell cycle or maintaining a progenitor phenotype varies according to the age and upon different physiological and pathological extrinsic stimuli.

Discussion

We examined the distribution of stage-specific markers in newborn OPCs as well as early cell fates with the aim to shed light on the mechanisms underlying the persistence of OPCs within the adult CNS parenchyma, and to investigate the occurrence of OPC divisions with asymmetric features. Our results highlighted the existence of pairs of newborn OPCs endowed with distinct properties and short-term destinies. Diversity appeared as early as cells exited cytokinesis, but did not emerge from the asymmetric segregation of molecules such as NG2 or PDGFRa expressed in the mother cell. Rather, rapid downregulation of OPC markers and upregulation of molecules associated with cell cycle exit contributed to generate early sister OPC asymmetry. Our observations also indicated that both physiological and pathological factors affect the early phenotype of the OPC progeny.

Newborn sister OPCs have distinct immunophenotypic profiles and short-term fates

Our analysis showed that, at all examined ages, one day after their birth, OPC pairs existed where both, none or only one sister cell express typical progenitor markers, such as NG2, PDGFRa, Sox2 and Hes5, or molecules associated to cell cycle exit, such as the GPR17 receptor. Of note, in contrast to NG2 and PDGFRa, at this stage Sox2, Hes5 and GPR17 were detected in a minor fraction of newborn OPCs, suggesting that they identify specific subsets or functional stages among the OPC progeny. In line with this view, within newborn cells, the expression of Sox2 and GPR17 appeared largely segregated. These two markers were also often distributed in a complementary manner in sister OPCs, thereby unveiling the occurrence of phenotypic asymmetry in cells derived from the same mother OPC. Such an early molecular heterogeneity, together with the occurrence of phenotypic asymmetry between sister cells, diverges from the proposed view that OPC proliferation produces cell pairs with identical properties (Hughes et al., 2013). Our results

show that newborn OPCs are not all molecularly equal, and suggest that, either as a response to environmental factors or as the result of intrinsic mechanisms, this heterogeneity may confer a dissimilar propensity toward re-entry into the cell cycle or maturation. Notably, in line with previous studies (Zhu et al., 2011; Dawson et al., 2003), phenotypic diversity in OPC pairs was also found over time, when a significant fraction of GPR17+ cells started to co-express premyelinating markers and cells re-entering the cell cycle were consistently GPR17-negative. Thus, early phenotypic differences occurring soon after mitosis anticipate distinct short-term behaviours of sister OPCs. However, the precise correlation between early marker expression and ultimate OPC destinies remains to be definitively assessed. Namely, our data show that about one third of GPR17+ cells acquire premyelinating features soon after mitosis. Yet, we cannot predict whether, when and how many of the other cells initially expressing GPR17 actually proceed towards terminal differentiation. The present data indicate that they are quiescent and, at least with our protocol of EdU administration, they do not appear to re-enter the cell cycle. However, we cannot exclude that, after experiencing a GPR17+ phase, a fraction of cells may downregulate the receptor and re-acquire progenitor features at later time points. GPR17+ cells may thus represent a transient non-mitotic stage that persist for very long periods until cells proceed toward differentiation or re-enter cell cycle according to the environmental needs. Consistently, two-photon imaging of adult NG2+ cells *in vivo* showed that most differentiating oligodendrocytes in the intact cortex are not recently generated and highlighted a remarkable heterogeneity of oligodendroglial maturation rates (Hughes et al., 2013). Previous studies have reported that cells have to downregulate GPR17 before acquiring myelin proteins (Boda et al., 2011; Fumagalli et al., 2011) and that forced expression of the receptor in oligodendroglia inhibits terminal maturation (Chen et al., 2009; Daniele et al., 2014). Of note, GPR17 expression on cell surface is regulated by extrinsic signals, indicating a prominent role of environmental cues in determining the

length of the GPR17+ phase (Fratangeli et al., 2013; Daniele et al., 2014). Further, we found that about a third of the newborn OPCs re-enter cell cycle after 7 days in the juvenile cortex. These data do not exclude the possibility that some cells displaying progenitor features within the time window of our analysis could be engaged in differentiation at later time points. Moreover, some of the newborn cells could undergo cell death, as has recently been shown (Hughes et al., 2013). Lineage tracing approaches, including the generation of novel CreERT mouse lines, are required to assess the terminal fate of OPC subsets endowed with distinct immunophenotypic profiles early after cell birth.

Downregulation and upregulation mechanisms contribute to sister OPC diversity

Diversity of NSC progeny is reportedly generated by the asymmetric segregation of RNAs and proteins in the two prospective daughter cells during mitosis (Knoblich et al., 2010). In the case of OPCs, Sugiarto and colleagues (2011) showed that NG2 segregates asymmetrically in adult mitotic OPCs *in vitro* to generate sister cells endowed with distinct fates. Conversely, previous *in vivo* analysis at postnatal ages and time-lapse imaging in the adult cortex described symmetric OPC divisions (Kukley et al., 2008; Hughes et al., 2013). Here, we found that in the juvenile cortex NG2 and PDGFRa never segregated asymmetrically *during* OPC mitosis. Rather, in a fraction of sister OPC pairs they appeared rapidly and asymmetrically downregulated *after* cytokinesis. Similar results were obtained *in vitro* in mitotic primary OPCs even in conditions expected to enhance asymmetry, as those promoting the appearance of mixed clones including OPCs and premyelinating cells. Yet, NG2+ endosome-like intracellular granules appeared to be asymmetrically distributed in a subset of OPCs in telophase, suggesting that sister OPC diversity relied onto a precocious degradation of this progenitor marker. Thus, our data indicate that diversity in daughter OPCs derives from the downregulation and degradation of membrane determinants of the progenitor state rather than on their polarized distribution to the

progeny. These results agree with the absence of NG2 segregation during OPC mitosis as shown in a recent *in vivo* imaging study where OPCs were visualized by eGFP positivity driven by the NG2 promoter (Hughes et al., 2013). However, at difference with this study, our data also show the emergence of pairs of NG2+ and NG2-negative sister cells soon after cell birth, in line with other former findings (Sugiarto et al. 2011). The stability of the eGFP reporter employed by Hughes et al. (2013) might have masked the precocious regulation of NG2 levels detected in our analysis.

On the whole, our results indicate that sister OPC diversity emerges from i) NG2 and PDGFRa downregulation occurring early after cell division, and ii) upregulation of molecules associated to cell cycle exit and transition to further stages in the lineage (i.e. GPR17) during the late phases of OPC mitosis. These events may be determined by the cell response to contact-mediated mechanisms, as suggested by proximity of diverse sister cells and by NSC studies (Lu et al., 2000), and/or by other extrinsic cues (see also below). Yet, *in vitro* evidence points to a certain degree of cell autonomous regulation in the emergence of sister OPC diversity. Indeed, downregulation/upregulation dynamics found in our study could occur as a consequence of the segregation of other molecules in cycling OPCs. Interestingly, NG2+ cells have been shown to express molecular regulators of polarity and cell fate determinants known to be asymmetrically distributed during NSC divisions (Binamé et al., 2013; Givogri et al., 2003; see also Suppl. Fig. 5). Whether sister OPC diversity relies on these molecular mechanisms remains to be investigated.

Intrinsic and extrinsic factors influence early heterogeneity of sister OPCs in vivo

Studies on NSCs showed that progenitor division mode and progeny commitment to distinct fates can be affected by various intrinsic and extrinsic factors. Interestingly, we found that proceeding from postnatal to adult stages the fraction of asymmetric OPC pairs significantly increased. Though fractions of symmetric and asymmetric OPC pairs varied

with age, their concomitant existence prompts the question of whether they arise either i) from distinct types of mother OPCs intrinsically committed to generate homogeneous or heterogeneous progenies, or ii) from plastic adaptation to environmental requirements. Hence, amplification of sister OPC asymmetry at adult age may result either from the expansion of a particular subset of mother OPCs, or from environmental conditions inhibiting exponential OPC production. Notably, pioneer studies in the field (Wren et al., 1992; Yakolev et al., 1996) showed that OPCs *in vitro* become competent to generate asymmetric daughter cells only after they have completed a critical number of mitotic cycles. According to this view, cycling OPCs *in vivo* that produce either symmetric or asymmetric progeny may be cells that had proliferated a different number of times. Consistently, symmetry of OPC progeny may prevail at early postnatal stages, while sister cell diversity may increase in the adult cortex, as a consequence of the progressive accumulation of OPCs that had reached a critical number of symmetric self-renewing divisions.

Of note, at old age, marker asymmetry in sister OPCs appeared significantly reduced and newborn cells maintained progenitor features with higher frequency compared to earlier adult stages. The lack of a further expansion of the asymmetric subset indicates that factors other than accumulation of cell cycles are influencing cycling OPCs at this stage. The progressive reduction of OPC maturation capacity/rate during aging (van Wijngaarden and Franklin, 2013) may account for the prevalence of pairs that are symmetric for progenitor features. Interestingly, studies in *Drosophila* and in the mammalian hematopoietic system indicated a correlation between altered stem cell polarity and stem cell aging. Dramatic changes in the expression levels of some master regulators of polarity and asymmetric division were reported in aged stem cells impairing both self-renewal and progeny differentiation (Florian and Geiger, 2010; Yamashita et al., 2010).

As regards pathological stimuli, we found that sister OPCs generated after traumatic or demyelinating injury rapidly upregulated markers of cell cycle exit (i.e. GPR17) in a symmetric manner, suggesting that lesions precociously engage OPCs in lineage progression. In a complementary way, expression of the same marker appeared significantly reduced compared to WT, in sister OPC pairs born in the context of reduced oligodendrocyte death (i.e. the juvenile p53-KO mouse cortex; Eizenberg et al., 1995; Li et al., 2008). However, the OPC asymmetric fraction did not vary in either condition. Thus, injury-related factors and turnover-related cues deeply affect the early phenotype of newborn OPCs by shifting the population toward either lineage progression or maintenance of progenitor features.

Upon enhanced voluntary physical exercise, markers associated with the transition to further lineage stages appeared precociously induced in newborn cells. This result is in line with previous findings (Simon et al., 2011) and suggests that physiological variations of neuronal activity modulate the fate of the OPC progeny as early as cells exit mitosis. Interestingly, at difference with injury-induced mechanisms, running boosted OPC cell cycle exit by expanding the fraction of sister cells asymmetric for GPR17. Of note, within the SGZ physical exercise was shown to preferentially affect the functions of selected subpopulations of NSCs (Lugert et al., 2010). Whether running, as well as the other examined stimuli, also differentially operates on defined subsets - if they exist - of parenchymal OPCs able to divide either symmetrically or asymmetrically remains to be elucidated.

Notably, in all these last experimental models PDGFRa distribution in newborn OPC pairs did not vary significantly compared to control conditions. This may reflect different kinetics of PDGFRa downregulation and GPR17 induction or, alternatively, may indicate that PDGFRa expression in OPCs is exclusively regulated by cell intrinsic mechanisms.

In conclusion, our study shows that cycling OPCs in the adult and juvenile cortex give rise to both homogenous and heterogeneous pairs of daughter cells. Diversity in the OPC progeny consists in early phenotypic differences and distinct short-term fates. We further provide mechanistic insights into OPC division by showing how downregulation of progenitor markers and induction of molecules associated with lineage progression participate in generating sister OPC diversity, and show that environmental factors modulate the early phenotype of the OPC progeny. Identifying precocious cell-autonomous and extrinsic factors contributing to determine the fate of the OPC progeny is expected to expand our understanding of the mechanisms by which NG2+ progenitors are maintained in the adult CNS.

Acknowledgements

The work of Enrica Boda and Annalisa Buffo is supported by the Italian Ministry for University and Research (MIUR, PRIN 20107MSMA4 to AB). Enrica Boda was supported by a postdoctoral fellowship of the Giuseppe Levi Foundation, Accademia Nazionale dei Lincei, Italy, and is currently recipient of a postdoctoral fellowship granted by the Umberto Veronesi Foundation, Italy. The work of Patrizia Rosa is supported by Cariplo Foundation (ref. 2012 0546 to PR). Maria P. Abbracchio is grateful to Fondazione Italiana Sclerosi Multipla (FISM2010/R1 and FISM2013/R1). We thank Chiara Rolando, Marco Sassoè, Ferdinando Di Cunto, Leda Dimou and Francesca Viganò for helpful comments on the manuscript. We are also grateful to Miltenyi Biotec for help with cell separation and to Bernard Zalc for the generous gift of the anti-PLP/DM20 antibody.

Figure legends

Figure 1. Markers associated to the progenitor phenotype or the cell cycle exit are heterogeneously expressed in pairs of sister OPCs early after cell division

(A-O) At 1 day post-BrdU administration (1 dpi), pairs of BrdU-retaining (red) OPCs were found in the juvenile (P20) mouse cortex where the expression of NG2 (green in A-C), PDGFRa (green in D-F), Sox2 (green in G-I), Hes5 (Hes5-GFP; green in J-L) and GPR17 (green in M-O) pertained to both (A,D,G,J,M), none (C,F,I,L,O) or only one sister cell (B,E,H,K,N). Yellow arrowheads in (A-O) indicate cells expressing the markers. White arrowheads indicate negative cells. Scale bars: 20 μm. (P,Q) Frequencies of the BrdU-retaining OPC pairs found symmetrically positive, asymmetric or symmetrically negative for the above-cited markers in the adult (P) and juvenile (Q) cortex. (R) Diagram of PDGFRa, GPR17 and Sox2 colocalization in BrdU+ OPC pairs at 1 dpi in P20 mouse cortex. (S) Colocalization analysis of the OPC pairs where GPR17 was asymmetrically distributed in only one of the two sister cells. Black dots in (P-S) represent marker positivity, while white dots correspond to absence of marker expression.

Figure 2. Activity of the NG2 promoter in newly-generated OPC pairs

Adult NG2CreERTM;R26YFP mice were first given BrdU to label pairs of sister OPCs and than received tamoxifen at 1 and 2 days after BrdU injection to mark NG2 actively transcribing cells. After 14 days, pairs of BrdU (red)-retaining OPCs were detected where both (A), none (B) or only one sister cell displayed YFP positivity (green). Within this class of asymmetric OPC pairs, GPR17 (blue in D) was mostly expressed by YFP-negative cells, while PDGFRa (blue in E) appeared more frequently in YFP+ sister OPCs ($P<0.001$ Chi-square test, PDGFRa compared to GPR17 distribution). Yellow arrowheads in (A-E) indicate YFP+ cells; white arrowheads indicate YFP-negative ones. Scale bars: 20 μm.

Figure 3. Immunophenotypic profile of BrdU-retaining sister OPCs at 7 days post-BrdU injection in the juvenile (P20) cortex

(A) Frequencies of BrdU-retaining OPC pairs positive, asymmetric or negative for distinct progenitor and maturation markers at 7 dpi. (B) Diagram of PDGFRa, GPR17, Nkx2.2 and PLP/DM20 colocalization in BrdU+ OPCs in pairs. (C) Colocalization analysis of the OPC pairs where GPR17 was asymmetrically distributed in only one of the two sister cells. (D, E) While PDGFRa (green in D) was expressed predominantly by GPR17 (blue in D, E) – negative BrdU (red)-retaining sister OPCs, the premyelinating marker PLP/DM20 (green in E) mostly colocalized with the receptor. Yellow arrowheads (D,E): GPR17-positive cells; white arrowheads: receptor negative cells. Scale bars: 20 μm. Black dots in (A,C) represent marker positivity, while white dots correspond to absence of marker expression.

Figure 4. Asymmetric re-proliferation of BrdU-retaining OPC pairs at 7 days post-BrdU injection in the juvenile (P20) cortex

(A-D, F) 7 days after receiving BrdU, P20 mice were given a 2 hours pulse of EdU to label cells re-entering cell cycle at this stage and then sacrificed. BrdU (red) retaining OPC pairs where none (A), both (B) or only one sister cell (C,D) incorporated EdU (white) were found. Yellow arrowheads in (A-C): EdU+ cells; white arrowheads: EdU negative cells. (E) Size of BrdU-retaining OPC clusters at 7dpi. (F) Analysis of GPR17 co-expression in EdU-asymmetrically incorporating OPC pairs. Black dots represent marker positivity, while white dots correspond to absence of marker expression. (G) BrdU (red)-retaining sister cells expressing GPR17 (blue) displayed high levels of p27/kip1 (green). Scale bars: 20 μm.

Figure 5. Immunophenotypic asymmetry of sister OPCs persists for months in the adult cortex

(A) At 7 days post-tamoxifen administration, YFP (green)-positive OPC pairs were frequently found in the cortex (indicated by white arrowheads). (B-E) At 5 weeks post-tamoxifen administration, YFP (green)-labeled OPC pairs were found where none (A), both (D) of only one (C) sister cell displayed GPR17 (red) positivity. (E) YFP+ clusters including 3 cells were also found, that often included only one GPR17+ OPC. Yellow arrowheads in (B-E) indicate GPR17+ cells; white arrowheads point to receptor negative cells. (F) At 11 weeks post-tamoxifen administration, YFP (green)+ OPC pairs were detected where the expression of the mature oligodendrocyte marker GST-pi (red) pertained to only one sister cell. In GST-pi-positive cells YFP labelled small round-shaped somata while in GST-pi-negative OPCs (white arrowhead) appeared ramified cells with larger and elongated cell bodies. Scale bars: 20 μm.

Figure 6. PDGRa, NG2 and GPR17 expression at OPC mitosis

(A-K) PDGFRa (red in A, C, F, H, J, K), NG2 (red in B, D, E, G, I) and GPR17 (green in A, C, D, F-J) distributions were investigated in OPCs undergoing distinct mitotic phases, based on chromatin (DAPI, blue) organization and nuclear envelope (labeled by anti-LMNB1 antibody, green in B,E) appearance (P20). Both PDGFRa and NG2 were found homogenously expressed on cell membranes during prophase (i.e. DNA compaction in grains and initial disorganization of LMNB1-labeled nuclear envelope; A, B) and metaphase (i.e. highly condensed chromatin disposed on the metaphasic plate; C,D). At this stage, GPR17 was not expressed by OPCs (A, C, D). OPCs undergoing anaphase (i.e. highly condensed chromatin distributed at the two poles, but still included in a unique nuclear envelope; E) or telophase (i.e. highly condensed chromatin distributed at the two poles with formation of a membranous PDGFRa- and NG2- enriched septum between the two cells; F,G) still expressed PDGFRa and NG2 on the whole cell body surface. (F-H) GPR17-labeled intracellular spots (arrowheads) appeared in a fraction of OPCs

undergoing telophase, and were often distributed asymmetrically in only one of the two prospective daughter cells. (I) GPR17+ accumulations were found also in a fraction of OPC pairs that just exited cytokinesis (i.e. juxtaposed and specular separate cell somata with decompacting grainy DNA; H-K). (I, K) NG2 and PDGFRa appeared unevenly distributed in the two daughter cells post-citokinesis (arrowhead in K: PDGFRa-maintaing sister cell). (L) Frequencies of BrdU-retaining OPC pairs found symmetrically positive, asymmetric or symmetrically negative for PDGFRa and GPR17 at 4 hours after BrdU-injection. Black dots in the legend of (L) represent marker positivity, while white dots correspond to absence of marker expression. (M-S) NG2 (green) distribution in mitotic OPCs in vitro. During the entire progression of the mitotic phases, NG2 appeared homogeneously distributed on the cell surface. (R, S) Cells with intracellular NG2 accumulations (white arrowheads) reminiscent of endosomes. Such vesicle-like structures appeared asymmetrically segregated in a fraction of OPCs (S). Scale bars: 5 μm.

Figure 7. Intrinsic and extrinsic factors modulate the immunophenotypic prolife of sister OPCs early after cell birth

(A-J) Effects of distinct physiological and pathological stimuli on OPC proliferation rate and PDGFRa or GPR17 distributions in BrdU-retaining OPC pairs at 1 day after BrdU injection. (A-C) In transition from early postnatal to adult stages, OPC proliferation rate declines (A) and a significant variation occurs in the frequencies of OPC pairs symmetric/asymmetric for PDGFRa (B) and GPR17 (C). Asterisks (A): P-values obtained in One-way Anova. (B,C) Asterisks: P-values obtained by Chi-square test analysis of marker distributions at different ages. (D-G) Upon both stab-wound cortical injury (grey matter; D,E) and LPC-induced focal demyelination (subcortical white matter; F,G), the number of newly-generated OPCs significantly increased (D,F; $P< 0.01$ SW or LPC vs. intact condition) in parallel with a significant change of the frequencies of GPR17-

expressing OPC pairs (P<0,001 SW or LPC vs. intact condition, Chi-square test; E,G). (H) Higher levels of voluntary motor activity (running wheel) were associated with a moderate decrease in OPC proliferation rate (P<0.05 running vs. standard conditions) and a significant reduction of the GPR17-negative OPC pair fraction (P<0.01 running vs. standard conditions, Chi square test analysis; I). (L) Reduced OPC proliferation (P<0.05 p53-ko vs. WT, t-test; L) in juvenile (P20) p53-KO mice. (J) GPR17-negative OPC pairs significantly increased in p53-KO (P<0.05 p53-KO vs. WT, t-test and Chi square test analysis on the OPC pair frequency distributions; J). Black dots in the legend of (B,C,E,G,I,J) represent marker positivity, while white dots correspond to absence of marker expression. *, P<0.05; **, P<0.01; ***, P<0,001.

References

Agathou S, Káradóttir RT, Kazanis I. 2013. Niche derived oligodendrocyte progenitors: a source of rejuvenation or complementation for local oligodendrogenesis? Front Cell Neurosci 7:188.

Barres BA, Raff MC, Gaese F, Bartke I, Dechant G, Barde YA. 1994. A crucial role for neurotrophin-3 in oligodendrocyte development. Nature 367:371-5.

Binamé F, Sakry D, Dimou L, Jolivel V, Trotter J. 2013. NG2 regulates directional migration of oligodendrocyte precursor cells via Rho GTPases and polarity complex proteins. J Neurosci 33:10858-74.

Boda E, Viganò F, Rosa P, Fumagalli M, Labat-Gest V, Tempia F, Abbracchio MP, Dimou L, Buffo A. 2011. The GPR17 receptor in NG2 expressing cells: focus on in vivo cell maturation and participation in acute trauma and chronic damage. Glia 59:1958-73.

Buffo A, Vosko MR, Erturk D, Hamann GF, Jucker M, Rowitch D, Gotz M. 2005. Expression pattern of the transcription factor Olig2 in response to brain injuries: implications for neuronal repair. Proc Natl Acad Sci U S A 102:18183-18188.

Chen Y, Wu H, Wang S, Koito H, Li J, Ye F, Hoang J, Escobar SS, Gow A, Arnett HA, Trapp BD, Karandikar NJ, Hsieh J, Lu QR. 2009. The oligodendrocyte-specific G protein-coupled receptor GPR17 is a cell-intrinsic timer of myelination. Nat Neurosci 12:1398-1406.

Ciana P, Fumagalli M, Trincavelli ML, Verderio C, Rosa P, Lecca D, Ferrario S, Parravicini

C, Capra V, Gelosa P, Guerrini U, Belcredito S, Cimino M, Sironi L, Tremoli E, Rovati GE, Martini C, Abbracchio MP. 2006. The orphan receptor GPR17 identified as a new dual uracil nucleotides/cysteinyl-leukotrienes receptor. EMBO J 25:4615-4627.

Corsini NS, Sancho-Martinez I, Laudenklos S, Glagow D, Kumar S, Letellier E, Koch P, Teodorczyk M, Kleber S, Klussmann S, Wiestler B, Brüstle O, Mueller W, Gieffers C, Hill O, Thiemann M, Seedorf M, Gretz N, Sprengel R, Celikel T, Martin-Villalba A. 2009. The death receptor CD95 activates adult neural stem cells for working memory formation and brain repair. Cell Stem Cell 5:178-90.

Daniele S, Trincavelli ML, Fumagalli M, Zappelli E, Lecca D, Bonfanti E, Campiglia P, Abbracchio MP, Martini C. 2014. Does GRK-β arrestin machinery work as a "switch on" for GPR17-mediated activation of intracellular signaling pathways? Cell Signal 26:1310-25.

Dawson MR, Polito A, Levine JM, Reynolds R. 2003. NG2-expressing glial progenitor cells: an abundant and widespread population of cycling cells in the adult rat CNS. Mol Cell Neurosci 24:476-88.

Durand B, Raff M. 2000. A cell-intrinsic timer that operates during oligodendrocyte development. Bioessays 22:64-71.

Eizenberg O, Faber-Elman A, Gottlieb E, Oren M, Rotter V, Schwartz M. 1995. Direct involvement of p53 in programmed cell death of oligodendrocytes. EMBO J 14:1136-44.

Encinas JM, Michurina TV, Peunova N, Park JH, Tordo J, Peterson DA, Fishell G, Koulakov A, Enikolopov G. 2011. Division-coupled astrocytic differentiation and age-related depletion of neural stem cells in the adult hippocampus. Cell Stem Cell 8:566-79.

Florian MC, Geiger H. 2010. Concise review: polarity in stem cells, disease, and aging. Stem Cells 28:1623-9.

Fratangeli A, Parmigiani E, Fumagalli M, Lecca D, Benfante R, Passafaro M, Buffo A, Abbracchio MP, Rosa P. 2013. The regulated expression, intracellular trafficking, and membrane recycling of the P2Y-like receptor GPR17 in Oli-neu oligodendroglial cells. J Biol Chem 288:5241-56.

Fumagalli M, Daniele S, Lecca D, Lee PR, Parravicini C, Fields RD, Rosa P, Antonucci F, Verderio C, Trincavelli ML, Bramanti P, Martini C, Abbracchio MP. 2011. Phenotypic changes, signaling pathway, and functional correlates of GPR17-expressing neural precursor cells during oligodendrocyte differentiation. J Biol Chem 286:10593-10604.

Givogri MI, Schonmann V, Cole R, De Vellis J, Bongarzone ER. 2003. Notch1 and Numb genes are inversely expressed as oligodendrocytes differentiate. Dev Neurosci 25:50-64.

Gonzalez-Perez O, Romero-Rodriguez R, Soriano-Navarro M, Garcia-Verdugo JM, Alvarez-Buylla A. 2009. Epidermal growth factor induces the progeny of subventricular zone type B cells to migrate and differentiate into oligodendrocytes. Stem Cells 27:2032-43.

Hill RA, Nishiyama A. 2014. NG2 cells (polydendrocytes): listeners to the neural network with diverse properties. Glia 62:1195-210.

Hughes EG, Kang SH, Fukaya M, Bergles DE. 2013. Oligodendrocyte progenitors balance growth with self-repulsion to achieve homeostasis in the adult brain. Nat Neurosci 16:668-76.

Jacks T, Remington L, Williams BO, Schmitt EM, Halachmi S, Bronson RT, Weinberg RA. 1994. Tumor spectrum analysis in p53-mutant mice. Curr Biol 4:1-7.

Knoblich JA. 2010. Asymmetric cell division: recent developments and their implications for tumour biology. Nat Rev Mol Cell Biol 11:849-60.

Kondo T, Raff M. 2000. Basic helix-loop-helix proteins and the timing of oligodendrocyte differentiation. Development 127:2989-98.

Kukley M, Kiladze M, Tognatta R, Hans M, Swandulla D, Schramm J, Dietrich D. 2008. Glial cells are born with synapses. FASEB J 22:2957-69.

Kukley M, Nishiyama A, Dietrich D. 2010. The fate of synaptic input to NG2 glial cells: neurons specifically downregulate transmitter release onto differentiating oligodendroglial cells. J Neurosci 30:8320-8331.

Li J, Ghiani CA, Kim JY, Liu A, Sandoval J, DeVellis J, Casaccia-Bonnefil P. 2008. Inhibition of p53 transcriptional activity: a potential target for future development of therapeutic strategies for primary demyelination. J Neurosci 28:6118-27.

Liu A, Li J, Marin-Husstege M, Kageyama R, Fan Y, Gelinas C, Casaccia-Bonnefil P. 2006. A molecular insight of Hes5-dependent inhibition of myelin gene expression: old partners and new players. EMBO J 25:4833-42.

Lu B, Jan L, Jan YN. 2000. Control of cell divisions in the nervous system: symmetry and asymmetry. Annu Rev Neurosci 23:531-56.

Lugert S, Basak O, Knuckles P, Haussler U, Fabel K, Götz M, Haas CA, Kempermann G, Taylor V, Giachino C. 2010. Quiescent and active hippocampal neural stem cells with distinct morphologies respond selectively to physiological and pathological stimuli and aging. Cell Stem Cell 6:445-56.

Ibarrola N, Mayer-Pröschel M, Rodriguez-Peña A, Noble M. 1996. Evidence for the existence of at least two timing mechanisms that contribute to oligodendrocyte generation in vitro. Dev Biol 180:1-21.

Maki T, Liang AC, Miyamoto N, Lo EH, Arai K. 2013. Mechanisms of oligodendrocyte regeneration from ventricular-subventricular zone-derived progenitor cells in white matter diseases. Front Cell Neurosci 7:275.

Menn B, Garcia-Verdugo JM, Yaschine C, Gonzalez-Perez O, Rowitch D, Alvarez-Buylla A. 2006. Origin of oligodendrocytes in the subventricular zone of the adult brain. J Neurosci 26:7907-18.

Nakatani H, Martin E, Hassani H, Clavairoly A, Maire CL, Viadieu A, Kerninon C, Delmasure A, Frah M, Weber M, Nakafuku M, Zalc B, Thomas JL, Guillemot F,Nait-Oumesmar B, Parras C. 2013. Ascl1/Mash1 promotes brain oligodendrogenesis during myelination and remyelination. J Neurosci 33:9752-68.

Rivers LE, Young KM, Rizzi M, Jamen F, Psachoulia K, Wade A, Kessaris N, Richardson WD. 2008. PDGFRA/NG2 glia generate myelinating oligodendrocytes and piriform projection neurons in adult mice. Nat Neurosci 11:1392-1401.

Robins SC, Villemain A, Liu X, Djogo T, Kryzskaya D, Storch KF, Kokoeva MV. 2013. Extensive regenerative plasticity among adult NG2-glia populations is exclusively based on self-renewal. Glia. 61:1735-47.

Simon C, Götz M, Dimou L. 2011. Progenitors in the adult cerebral cortex: Cell cycle properties and regulation by physiological stimuli and injury. Glia 59:869-881.

Sohn J, Natale J, Chew LJ, Belachew S, Cheng Y, Aguirre A, Lytle J, Nait-Oumesmar B, Kerninon C, Kanai-Azuma M, Kanai Y, Gallo V. 2006. Identification of Sox17 as a transcription factor that regulates oligodendrocyte development. J Neurosci 26:9722-35.

Srinivas S, Watanabe T, Lin CS, William CM, Tanabe Y, Jessell TM, Costantini F. 2001. Cre reporter strains produced by targeted insertion of EYFP and ECFP into the ROSA26 locus. BMC Dev Biol 1:4.

Sugiarto S, Persson AI, Munoz EG, Waldhuber M, Lamagna C, Andor N, Hanecker P, Ayers-Ringler J, Phillips J, Siu J, Lim DA, Vandenberg S, Stallcup W, Berger MS, Bergers

G, Weiss WA, Petritsch C. 2011. Asymmetry-defective oligodendrocyte progenitors are glioma precursors. Cancer Cell 20:328-40.

Tamura Y, Kataoka Y, Cui Y, Takamori Y, Watanabe Y, Yamada H. 2007. Intracellular translocation of glutathione S-transferase pi during oligodendrocyte differentiation in adult rat cerebral cortex in vivo. Neuroscience 148:535-540.

van Wijngaarden P, Franklin RJ. 2013. Ageing stem and progenitor cells: implications for rejuvenation of the central nervous system. Development 140:2562-75.

Walker AS, Goings GE, Kim Y, Miller RJ, Chenn A, Szele FG. 2010. Nestin reporter transgene labels multiple central nervous system precursor cells. Neural Plast 2010:894374.

Wren D, Wolswijk G, Noble M. 1992. In vitro analysis of the origin and maintenance of O-2A adult progenitor cells. J Cell Biol 116:167-76.

Yakovlev AY, Boucher K, Mayer-Proschel M, Noble M. 1998. Quantitative insight into proliferation and differentiation of oligodendrocyte type 2 astrocyte progenitor cells in vitro. Proc Natl Acad Sci U S A 95:14164-7.

Yamashita YM, Yuan H, Cheng J, Hunt AJ. 2010. Polarity in stem cell division: asymmetric stem cell division in tissue homeostasis. Cold Spring Harb Perspect Biol 2:a001313.

Young KM, Psachoulia K, Tripathi RB, Dunn SJ, Cossell L, Attwell D, Tohyama K, Richardson WD. 2013. Oligodendrocyte dynamics in the healthy adult CNS: evidence for myelin remodeling. Neuron 77:873-85.

Zhu X, Hill RA, Dietrich D, Komitova M, Suzuki R, Nishiyama A. 2011. Age-dependent fate and lineage restriction of single NG2 cells. Development 138:745-53.

Zhu Q, Zhao X, Zheng K, Li H, Huang H, Zhang Z, Mastracci T, Wegner M, Chen Y, Sussel L, Qiu M. 2014. Genetic evidence that Nkx2.2 and Pdgfra are major determinants of the timing of oligodendrocyte differentiation in the developing CNS. Development 141:548-55.

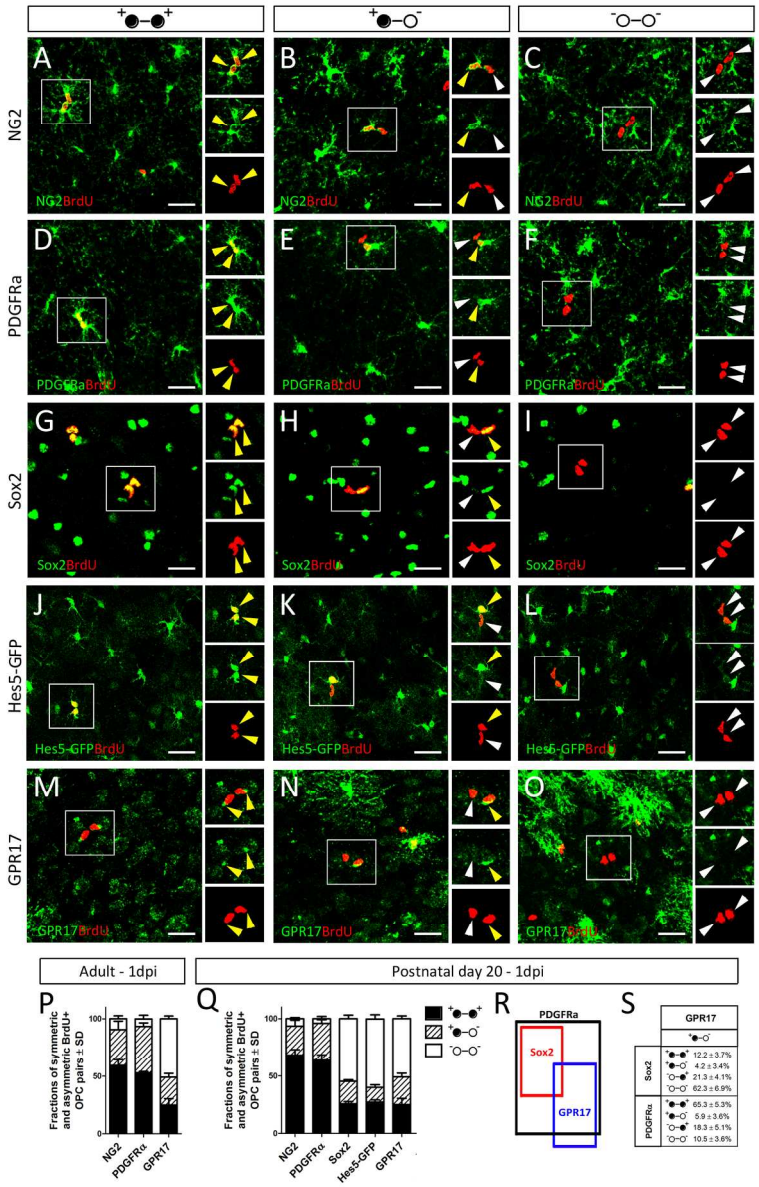

Figure 1. Markers associated to the progenitor phenotype or the cell cycle exit are heterogeneously expressed in pairs of sister OPCs early after cell division

(A-O) At 1 day post-BrdU administration (1 dpi), pairs of BrdU-retaining (red) OPCs were found in the juvenile (P20) mouse cortex where the expression of NG2 (green in A-C), PDGFRa (green in D-F), Sox2 (green in G-I), Hes5 (Hes5-GFP; green in J-L) and GPR17 (green in M-O) pertained to both (A,D,G,J,M), none (C,F,I,L,O) or only one sister cell (B,E,H,K,N). Yellow arrowheads in (A-O) indicate cells expressing the markers. White arrowheads indicate negative cells. Scale bars: 20 μm. (P,Q) Frequencies of the BrdU-retaining OPC pairs found symmetrically positive, asymmetric or symmetrically negative for the above-cited markers in the adult (P) and juvenile (Q) cortex. (R) Diagram of PDGFRa, GPR17 and Sox2 colocalization in BrdU+ OPC pairs at 1 dpi in P20 mouse cortex. (S) Colocalization analysis of the OPC pairs where GPR17 was asymmetrically distributed in only one of the two sister cells. Black dots in (P-S) represent marker positivity, while white dots correspond to absence of marker expression.

180x276mm (300 x 300 DPI)

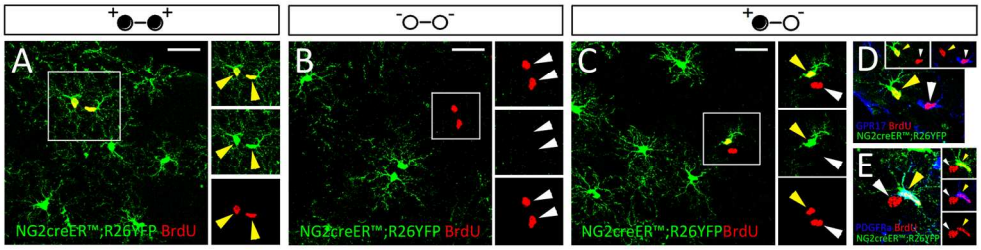

Figure 2. Activity of the NG2 promoter in newly-generated OPC pairs
Adult NG2CreERTM;R26YFP mice were first given BrdU to label pairs of sister OPCs and than received tamoxifen at 1 and 2 days after BrdU injection to mark NG2 actively transcribing cells. After 14 days, pairs of BrdU (red)-retaining OPCs were detected where both (A), none (B) or only one sister cell displayed YFP positivity (green). Within this class of asymmetric OPC pairs, GPR17 (blue in D) was mostly expressed by YFP-negative cells, while PDGFRa (blue in E) appeared more frequently in YFP+ sister OPCs ($P<0.001$ Chi-square test, PDGFRa compared to GPR17 distribution). Yellow arrowheads in (A-E) indicate YFP+ cells; white arrowheads indicate YFP-negative ones. Scale bars: 20 μm.
199x55mm (300 x 300 DPI)

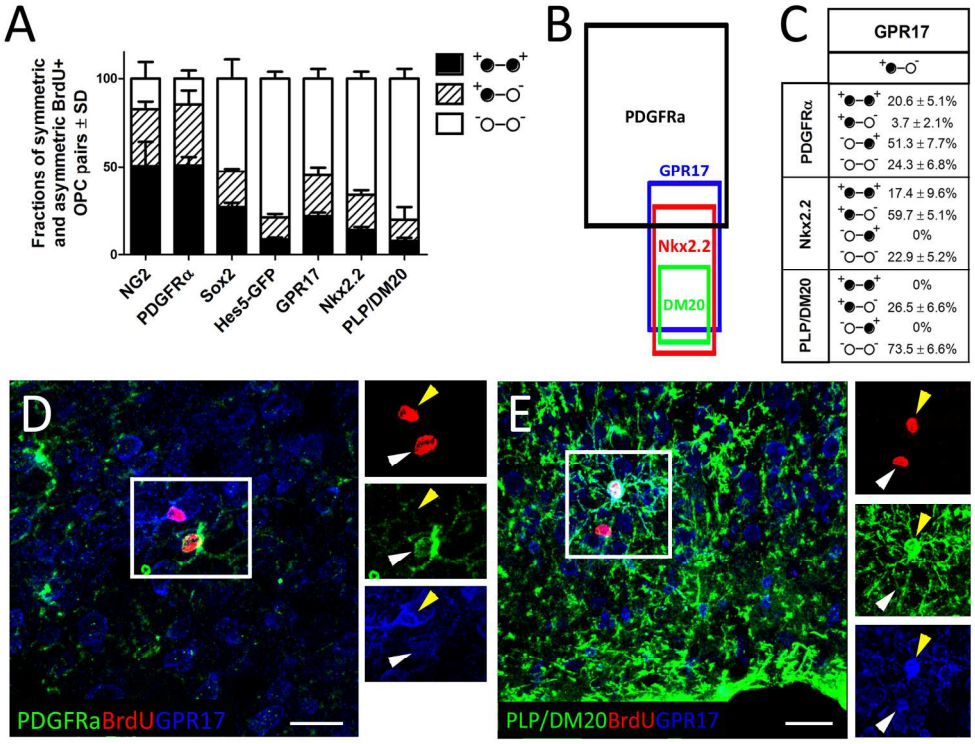

Figure 3. Immunophenotypic profile of BrdU-retaining sister OPCs at 7 days post-BrdU injection in the juvenile (P20) cortex

(A) Frequencies of BrdU-retaining OPC pairs positive, asymmetric or negative for distinct progenitor and maturation markers at 7 dpi. (B) Diagram of PDGFRa, GPR17, Nkx2.2 and PLP/DM20 colocalization in BrdU+ OPCs in pairs. (C) Colocalization analysis of the OPC pairs where GPR17 was asymmetrically distributed in only one of the two sister cells. (D, E) While PDGFRa (green in D) was expressed predominantly by GPR17 (blue in D, E) –negative BrdU (red)-retaining sister OPCs, the premyelinating marker PLP/DM20 (green in E) mostly colocalized with the receptor. Yellow arrowheads (D,E): GPR17-positive cells; white arrowheads: receptor negative cells. Scale bars: 20 μm. Black dots in (A,C) represent marker positivity, while white dots correspond to absence of marker expression.

180x139mm (300 x 300 DPI)

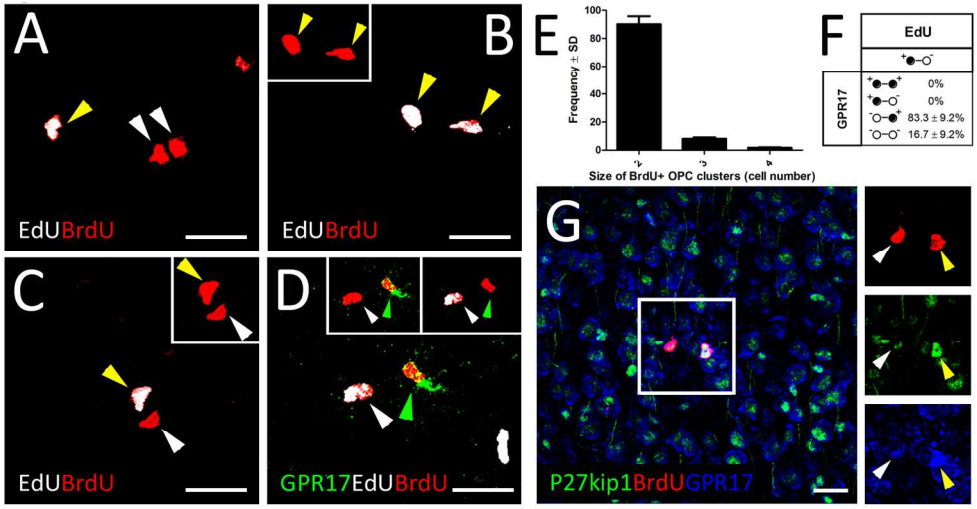

Figure 4. Asymmetric re-proliferation of BrdU-retaining OPC pairs at 7 days post-BrdU injection in the juvenile (P20) cortex

(A-D, F) 7 days after receiving BrdU, P20 mice were given a 2 hours pulse of EdU to label cells re-entering cell cycle at this stage and then sacrificed. BrdU (red) retaining OPC pairs where none (A), both (B) or only one sister cell (C,D) incorporated EdU (white) were found. Yellow arrowheads in (A-C): EdU+ cells; white arrowheads: EdU negative cells. (E) Size of BrdU-retaining OPC clusters at 7dpi. (F) Analysis of GPR17 co-expression in EdU-asymmetrically incorporating OPC pairs. Black dots represent marker positivity, while white dots correspond to absence of marker expression. (G) BrdU (red)-retaining sister cells expressing GPR17 (blue) displayed high levels of p27/kip1 (green). Scale bars: 20 μm.

159x85mm (300 x 300 DPI)

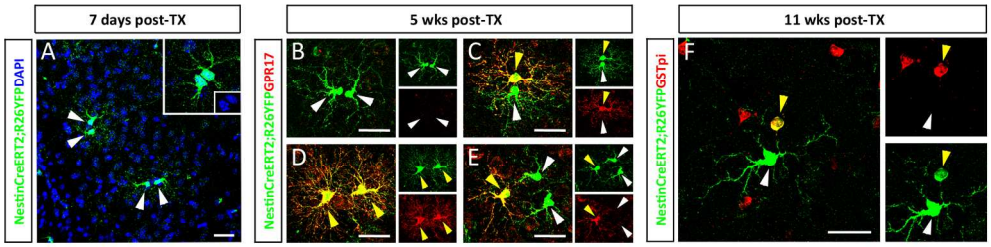

Figure 5. Immunophenotypic asymmetry of sister OPCs persists for months in the adult cortex
(A) At 7 days post-tamoxifen administration, YFP (green)-positive OPC pairs were frequently found in the cortex (indicated by white arrowheads). (B-E) At 5 weeks post-tamoxifen administration, YFP (green)-labeled OPC pairs were found where none (A), both (D) of only one (C) sister cell displayed GPR17 (red) positivity. (E) YFP+ clusters including 3 cells were also found, that often included only one GPR17+ OPC. Yellow arrowheads in (B-E) indicate GPR17+ cells; white arrowheads point to receptor negative cells. (F) At 11 weeks post-tamoxifen administration, YFP (green)+ OPC pairs were detected where the expression of the mature oligodendrocyte marker GST-pi (red) pertained to only one sister cell. In GST-pi-positive cells YFP labelled small round-shaped somata while in GST-pi-negative OPCs (white arrowhead) appeared ramified cells with larger and elongated cell bodies. Scale bars: 20 µm.
180x46mm (300 x 300 DPI)

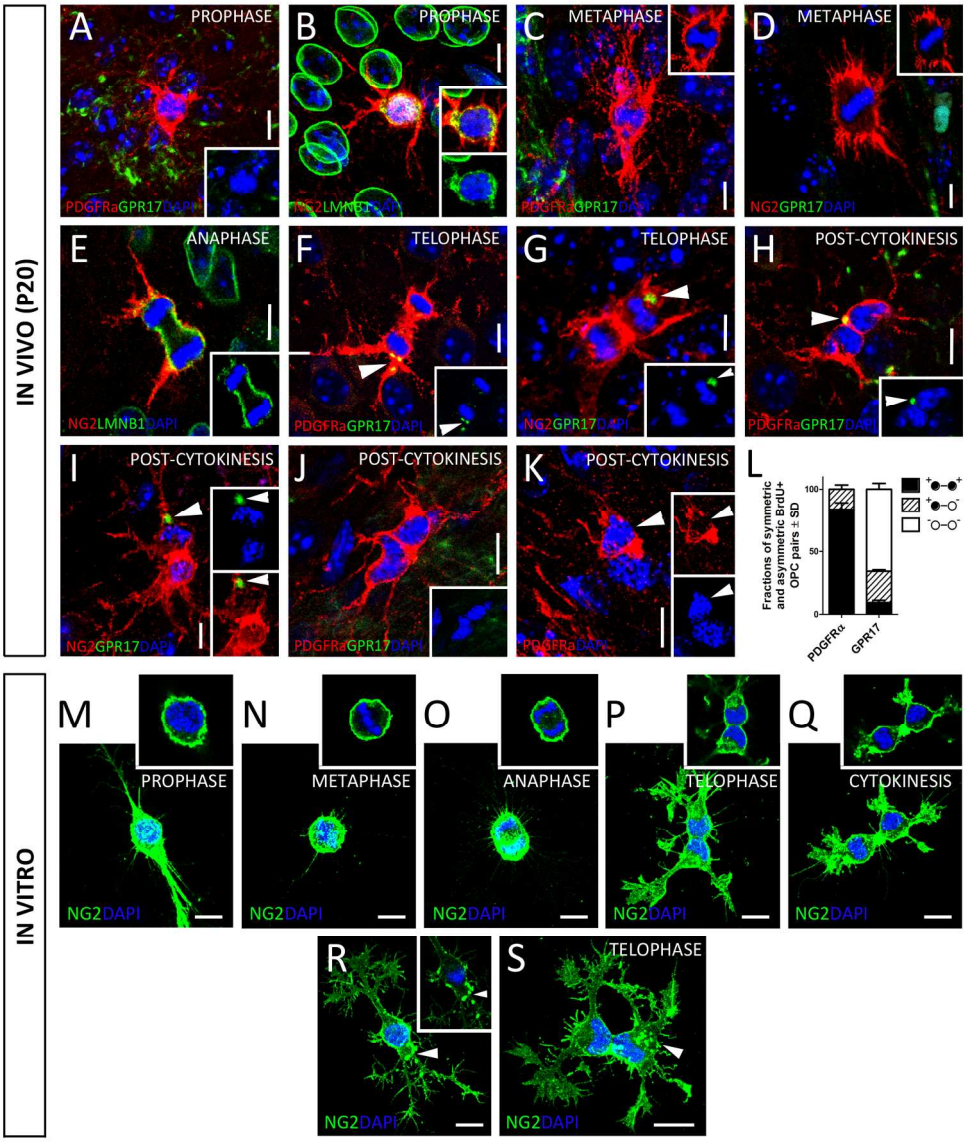

Figure 6. PDGRa, NG2 and GPR17 expression at OPC mitosis

(A-K) PDGFRa (red in A, C, F, H, J, K), NG2 (red in B, D, E, G, I) and GPR17 (green in A, C, D, F-J) distributions were investigated in OPCs undergoing distinct mitotic phases, based on chromatin (DAPI, blue) organization and nuclear envelope (labeled by anti-LMNB1 antibody, green in B,E) appearance (P20). Both PDGFRa and NG2 were found homogenously expressed on cell membranes during prophase (i.e. DNA compaction in grains and initial disorganization of LMNB1-labeled nuclear envelope; A, B) and metaphase (i.e. highly condensed chromatin disposed on the metaphasic plate; C,D). At this stage, GPR17 was not expressed by OPCs (A, C, D). OPCs undergoing anaphase (i.e. highly condensed chromatin distributed at the two poles, but still included in a unique nuclear envelope; E) or telophase (i.e. highly condensed chromatin distributed at the two poles with formation of a membranous PDGFRa- and NG2- enriched septum between the two cells; F,G) still expressed PDGFRa and NG2 on the whole cell body surface. (F-H) GPR17-labeled intracellular spots (arrowheads) appeared in a fraction of OPCs undergoing telophase, and were often distributed asymmetrically in only one of the two prospective daughter cells. (I) GPR17+ accumulations were found also in a fraction of OPC pairs that just exited cytokinesis (i.e. juxtaposed and specular separate

cell somata with decompacting grainy DNA; H-K). (I, K) NG2 and PDGFRa appeared unevenly distributed in the two daughter cells post-citokinesis (arrowhead in K: PDGFRa-maintaing sister cell). (L) Frequencies of BrdU-retaining OPC pairs found symmetrically positive, asymmetric or symmetrically negative for PDGFRa and GPR17 at 4 hours after BrdU-injection. Black dots in the legend of (L) represent marker positivity, while white dots correspond to absence of marker expression. (M-S) NG2 (green) distribution in mitotic OPCs in vitro. During the entire progression of the mitotic phases, NG2 appeared homogeneously distributed on the cell surface. (R, S) Cells with intracellular NG2 accumulations (white arrowheads) reminiscent of endosomes. Such vesicle-like structures appeared asymmetrically segregated in a fraction of OPCs (S). Scale bars: 5 μm.
180x209mm (300 x 300 DPI)

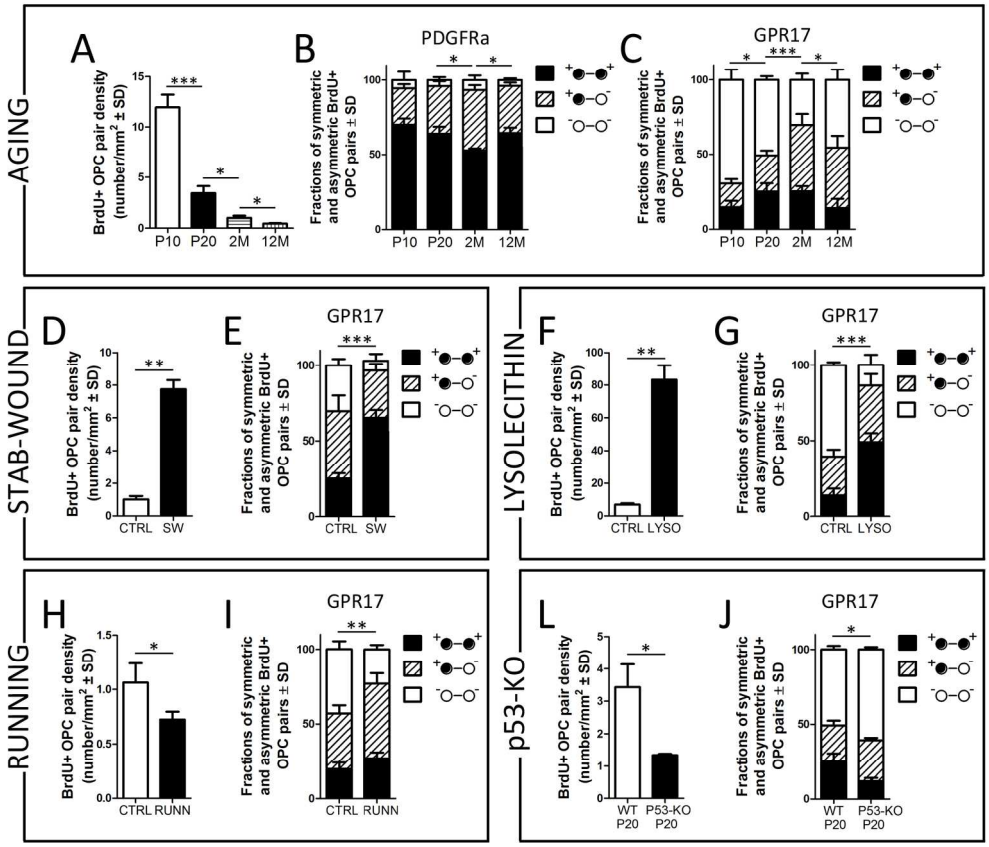

Figure 7. Intrinsic and extrinsic factors modulate the immunophenotypic prolife of sister OPCs early after cell birth

(A-J) Effects of distinct physiological and pathological stimuli on OPC proliferation rate and PDGFRa or GPR17 distributions in BrdU-retaining OPC pairs at 1 day after BrdU injection. (A-C) In transition from early postnatal to adult stages, OPC proliferation rate declines (A) and a significant variation occurs in the frequencies of OPC pairs symmetric/asymmetric for PDGFRa (B) and GPR17 (C). Asterisks (A): P-values obtained in One-way Anova. (B,C) Asterisks: P-values obtained by Chi-square test analysis of marker distributions at different ages. (D-G) Upon both stab-wound cortical injury (grey matter; D,E) and LPC-induced focal demyelination (subcortical white matter; F,G), the number of newly-generated OPCs significantly increased (D,F; P< 0.01 SW or LPC vs. intact condition) in parallel with a significant change of the frequencies of GPR17-expressing OPC pairs (P<0,001 SW or LPC vs. intact condition, Chi-square test; E,G). (H) Higher levels of voluntary motor activity (running wheel) were associated with a moderate decrease in OPC proliferation rate (P<0.05 running vs. standard conditions) and a significant reduction of the GPR17-negative OPC pair fraction (P<0.01 running vs. standard conditions, Chi square test analysis; I). (L) Reduced OPC proliferation (P<0.05 p53-ko vs. WT, t-test; L) in juvenile (P20) p53-KO mice. (J) GPR17-negative OPC pairs significantly increased in p53-KO (P<0.05 p53-KO vs. WT, t-test and Chi square test analysis on the OPC pair frequency distributions; J). Black dots in the legend of (B,C,E,G,I,J) represent marker positivity, while white dots correspond to absence of marker expression. *, P<0.05; **, P<0.01; ***, P<0,001.

180x159mm (300 x 300 DPI)

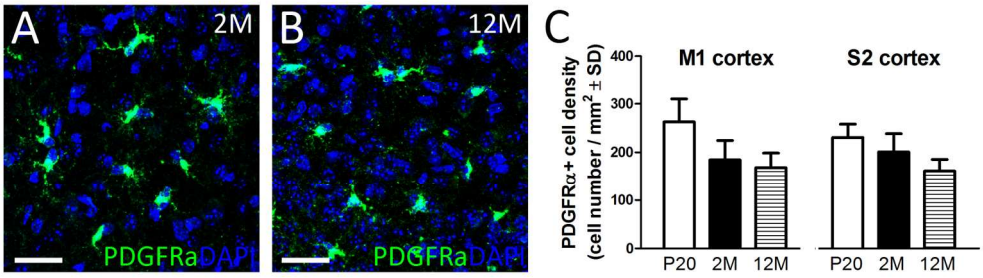

Supplementary Figure 1. PDGFRa-expressing cell density in juvenile, adult and old mouse cortices
(A,B) Representative images of PDGFRa (green)-expressing cells in the primary motor cortex (M1) of 2- and 12-months old mice. DAPI (blue) counterstains nuclei. Scale bars: 20 μm. (C) Histograms represent PDGFRa+ cell density in M1 and S2 (secondary somatosensitive) cortices at P20, 2 months and 12 months. In both regions after P20 PDGFRa+ OPC density did not vary significantly ($P>0.05$, One way Anova, $F=3.68$; $R2=0.4$).
167x51mm (300 x 300 DPI)

EXPERIMENTAL APPROACH/MODEL	METHOD	AIM
BrdU-based OPC pair analysis	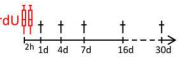	To tag and follow the fate of newly-generated OPC pairs
Hes-GFP	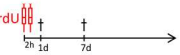	To assess the distribution of Hes5 (indicative of the activation of the canonical Notch pathway) in newly-generated OPC pairs
NG2creER^{TM};R26YFP	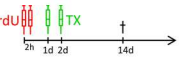	To assess the distribution of the NG2 promoter activity in newly-generated OPC pairs
Dual pulse labeling	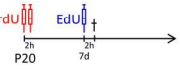	To tag cells re-entering cell cycle within the newly-generated OPC pairs
NestinCreERT2;R26YFP	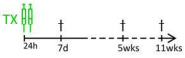	To tag and follow the long-term fate of the Nestin+ OPC progeny
CORTICAL STAB-WOUND	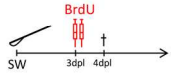	To assess whether injury-associated signals alter marker distribution in newly-generated OPC pairs
LYSOLECITHIN INJECTION	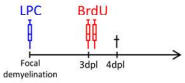	To assess whether injury-associated signals alter marker distribution in newly-generated OPC pairs
RUNNING WHEEL	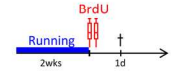	To assess whether increased levels of physical activity alter marker distribution in newly-generated OPC pairs
P53-KO		To assess whether a reduction in the physiological rate of oligodendrocyte cell death alters marker distribution in newly-generated OPC pairs

Supplementary Figure 2. In vivo and in vitro experimental models/approaches used in this study (A) In vivo experimental models. (B) In vitro experimental models. Black dots in (A) represent marker positivity, while white dots correspond to absence of marker expression. Abbreviations: h, hours; d, days; wks, weeks; TX, tamoxifen; SW, stab-wound; LPC, lysolecithin; dpl, days post-lesion.
167x240mm (300 x 300 DPI)

EXPERIMENTAL APPROACH/MODEL	METHOD	AIM
In vitro analysis 	In bFGF+PDGF: 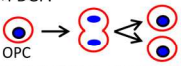 (Sohn et al., 2006; our clonal analysis) In PDGF or EGF+bFGF: 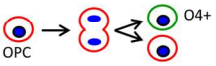 (Sohn et al., 2006; Ibarrola et al., 1996; Sugiarto et al., 2011; our clonal analysis)	To assess NG2 distribution during division of primary OPCs exposed to media that differentially modulate their differentiation probability while preserving cell proliferation
Gene expression analysis on acutely isolated OPCs	 **1.** Dissociation of P8 or P21 mouse cerebral cortex  **2.** Incubation with anti-PDGFRα or anti-AN2 antibodies conjugated to magnetic beads 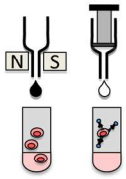 **3.** Magnetic cell sorting (Miltenyi system)  **4.** RNA extraction and RT-PCR	To investigate the expression of the mRNAs coding for cell fate determinants and regulators of division mode in OPCs acutely isolated from the cortical tissue

Supplementary Figure 2. In vivo and in vitro experimental models/approaches used in this study (A) In vivo experimental models. (B) In vitro experimental models. Black dots in (A) represent marker positivity, while white dots correspond to absence of marker expression. Abbreviations: h, hours; d, days; wks, weeks; TX, tamoxifen; SW, stab-wound; LPC, lysolecithin; dpl, days post-lesion.
167x184mm (300 x 300 DPI)

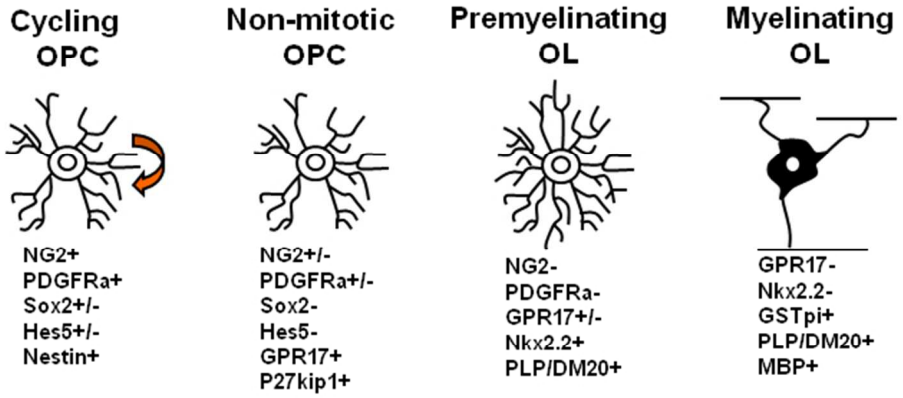

Supplementary Figure 3. Immunophenotype of cells along the oligodendroglial lineage. Representative scheme of the distinct phases of oligodendrocyte differentiation and related expression pattern. OPC, oligodendrocyte progenitor cell; OL, oligodendrocyte

184x88mm (96 x 96 DPI)

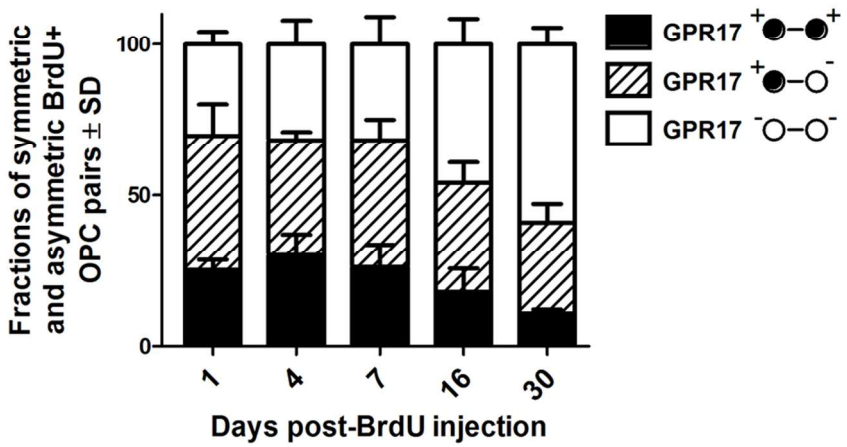

Supplementary Figure 4. Immunophenotypic profile of sister OPCs at late time points in the adult cortex Fractions of BrdU-retaining OPC pairs where GPR17 appeared symmetrically or asymmetrically expressed at distinct time points after BrdU-injection. Of note, GPR17 asymmetry persisted up to 30 dpi. Black dots in the legend represent marker positivity, while white dots correspond to absence of marker expression.

94x50mm (300 x 300 DPI)

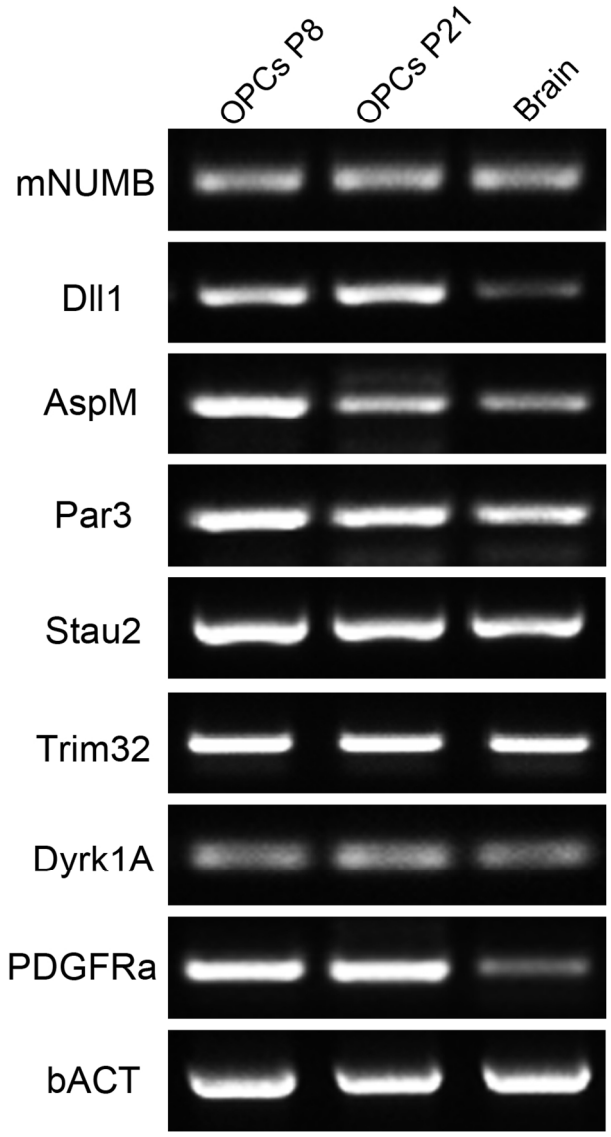

Supplementary Figure 5. Expression of fate determinants and polarity regulators in OPCs
OPCs acutely isolated by MACS technology from the postnatal (P8) and juvenile (P20) mouse cortex express transcripts for classical cell fate determinants and polarity machineries operating in NSC divisions. Such molecules include regulators of symmetric divisions (i.e. AspM; Fish et al., 2006), cell polarity organizers potentially implicated in asymmetric segregation of cell fate determinants during mitosis (i.e. Par3, Stau2; Knoblich, 2010; Kusek et al., 2012), modulators of EGFR (i.e. Dyrk1A) and canonical Notch pathways (i.e. Dll1 and mNUMB), which are known to segregate asymmetrically during NSC mitosis and operate as cell fate determinants (Knoblich et al., 2010; Ferron et al., 2010; Kawaguchi et al., 2013).

87x154mm (300 x 300 DPI)

Legends of Supplementary Figures

Supplementary Figure 1. PDGFRa-expressing cell density in juvenile, adult and old mouse cortices

(A,B) Representative images of PDGFRa (green)-expressing cells in the primary motor cortex (M1) of 2- and 12-months old mice. DAPI (blue) counterstains nuclei. Scale bars: 20 μm. (C) Histograms represent PDGFRa+ cell density in M1 and S2 (secondary somatosensitive) cortices at P20, 2 months and 12 months. In both regions after P20 PDGFRa+ OPC density did not vary significantly ($P>0.05$, One way Anova, $F=3.68$; $R^2=0.4$).

Supplementary Figure 2. In vivo and in vitro experimental models/approaches used in this study

(A) In vivo experimental models. (B) In vitro experimental models. Black dots in (A) represent marker positivity, while white dots correspond to absence of marker expression. Abbreviations: h, hours; d, days; wks, weeks; TX, tamoxifen; SW, stab-wound; LPC, lysolecithin; dpl, days post-lesion

Supplementary Figure 3. Immunophenotype of cells along the oligodendroglial lineage

Representative scheme of the distinct phases of oligodendrocyte differentiation and related expression pattern. OPC, oligodendrocyte progenitor cell; OL, oligodendrocyte

Supplementary Figure 4. Immunophenotypic profile of sister OPCs at late time points in the adult cortex

Fractions of BrdU-retaining OPC pairs where GPR17 appeared symmetrically or asymmetrically expressed at distinct time points after BrdU-injection. Of note, GPR17 asymmetry persisted up to 30 dpi. Black dots in the legend represent marker positivity, while white dots correspond to absence of marker expression.

Supplementary Figure 5. Expression of fate determinants and polarity regulators in OPCs

OPCs acutely isolated by MACS technology from the postnatal (P8) and juvenile (P20) mouse cortex express transcripts for classical cell fate determinants and polarity

machineries operating in NSC divisions. Such molecules include regulators of symmetric divisions (i.e. AspM; Fish et al., 2006), cell polarity organizers potentially implicated in asymmetric segregation of cell fate determinants during mitosis (i.e. Par3, Stau2; Knoblich, 2010; Kusek et al., 2012), modulators of EGFR (i.e. Dyrk1A) and canonical Notch pathways (i.e. Dll1 and mNUMB), which are known to segregate asymmetrically during NSC mitosis and operate as cell fate determinants (Knoblich et al., 2010; Ferron et al., 2010; Kawaguchi et al., 2013).

Supplementary references

Ferron SR, Pozo N, Laguna A, Aranda S, Porlan E, Moreno M, Fillat C, de la Luna S, Sánchez P, Arbonés ML, Fariñas I. 2010. Regulated segregation of kinase Dyrk1A during asymmetric neural stem cell division is critical for EGFR-mediated biased signaling. Cell Stem Cell 7:367-79.

Fish JL, Kosodo Y, Enard W, Pääbo S, Huttner WB. 2006. Aspm specifically maintains symmetric proliferative divisions of neuroepithelial cells. Proc Natl Acad Sci U S A 103:10438-43.

Kawaguchi D, Furutachi S, Kawai H, Hozumi K, Gotoh Y. 2013. Dll1 maintains quiescence of adult neural stem cells and segregates asymmetrically during mitosis. Nat Commun 4:1880.

Knoblich JA. 2010. Asymmetric cell division: recent developments and their implications for tumour biology. Nat Rev Mol Cell Biol 11:849-60.

Kusek G, Campbell M, Doyle F, Tenenbaum SA, Kiebler M, Temple S. 2012. Asymmetric segregation of the double-stranded RNA binding protein Staufen2 during mammalian neural stem cell divisions promotes lineage progression. Cell Stem Cell 11:505-16.